Coupled dynamics over the Indian Ocean: spring initiation of the Zonal Mode [☆]

H. Annamalai[a,*], R. Murtugudde[b], J. Potemra[a], S.P. Xie[a,c], P. Liu[a], B. Wang[a,c]

[a] *International Pacific Research Center, IPRClSOEST, University of Hawaii, 2525 Correa Road, Honolulu 96822, USA*
[b] *ESSIC, University of Maryland, College Park, MD, USA*
[c] *Department of Meteorology, SOEST, University of Hawaii, USA*

Abstract

Atmosphere and ocean model assimilated products, in conjunction with observed precipitation and ocean model estimates of Indonesian Throughflow (ITF) transport and barrier layer thickness, are analyzed to elucidate the role of external (ENSO and ITF) and internal (monsoon) factors in the initiation of the Indian Ocean Zonal Mode (IOZM).

The diagnostics show that there exists a natural mode of coupled variability in the eastern equatorial Indian Ocean (EEIO) that is weak on its own but intensifies in boreal spring/early summer, usually when ENSO-like conditions exist in the western Pacific, as implied by the Southern Oscillation Index (SOI). In the EEIO, there exists a *'time window'* in the annual cycle—boreal spring—during which the ocean–atmosphere system is particularly sensitive to external forcing. At interannual timescales, spring atmospheric conditions in the EEIO are remotely controlled by SST in the equatorial western-central Pacific. Warm SST anomalies there cause changes in the Pacific Walker circulation and induce subsidence over the EEIO that results in negative precipitation anomalies: (i) Forced by this heat sink, an anticyclone develops in the lower atmosphere over the southeastern Indian Ocean as a Rossby-wave response, and the alongshore upwelling-favorable winds off Java–Sumatra are enhanced. (ii) The reduced surface fresh-water flux and enhanced upwelling reduce the barrier layer in the upper ocean. These processes along-with the reduction of ITF help trigger the IOZM. Once triggered, IOZM grows in summer by the Bjerknes feedback. Its interactions with the monsoon heat source result in enhanced precipitation along the monsoon trough in July–August. This north–south heating gradient favors a local meridional circulation with increased alongshore winds off Sumatra, implying the potential role of the monsoon background cycle.

The hypothesis that the equatorial western-central Pacific SST anomalies control the spring precipitation variations in the EEIO/maritime continent is demonstrated by sensitivity experiments with an atmospheric general circulation model. During the spring initiation stages of the IOZM, an analysis of the mixed layer heat budget in an ocean general circulation model indicates that cooling off Java is primarily due to entrainment and also due to latent cooling, both caused by enhanced upwelling-favorable winds.

© 2003 Elsevier Science Ltd. All rights reserved.

1. Introduction

Understanding and modeling interannual SST variations in the equatorial Pacific associated with El Niño and the Southern Oscillation (ENSO)—

the backbone for seasonal to interannual climate prediction—have occupied the center stage of climate research for the last few decades (e.g., Philander, 1990; Wallace et al., 1998; Shukla, 1998). Early research showed the links between thermocline displacement, SST and zonal wind in the equatorial Pacific (Bjerknes, 1969). Unlike the central and eastern equatorial Pacific, the mean thermocline in the equatorial Indian Ocean is deep and flat with less upwelling on the annual mean, thereby limiting the effect of thermocline variability on SSTs, the main agent in the Bjerknes (1969) feedback loop. As a consequence, interannual SST fluctuations in most of the Indian

Ocean are modest ($<0.5°C$; Fig. 1a). Exceptions include three regions: southwest of Sumatra and Java, off Somalia, and the southwest tropical Indian Ocean (SWIO), where SST fluctuations are quite large.

Several studies using diversified methods (observations, ocean models, coupled ocean–atmosphere models) suggest that SST variability over the Indian Ocean is largely a response to ENSO through changes in net surface heat flux (Klein et al., 1999; Venzke et al., 2000) and in ocean circulation (Chambers et al., 1999; Schiller et al., 2000; Huang and Kinter, 2002). Xie et al. (2002) demonstrated the strong influence of subsurface
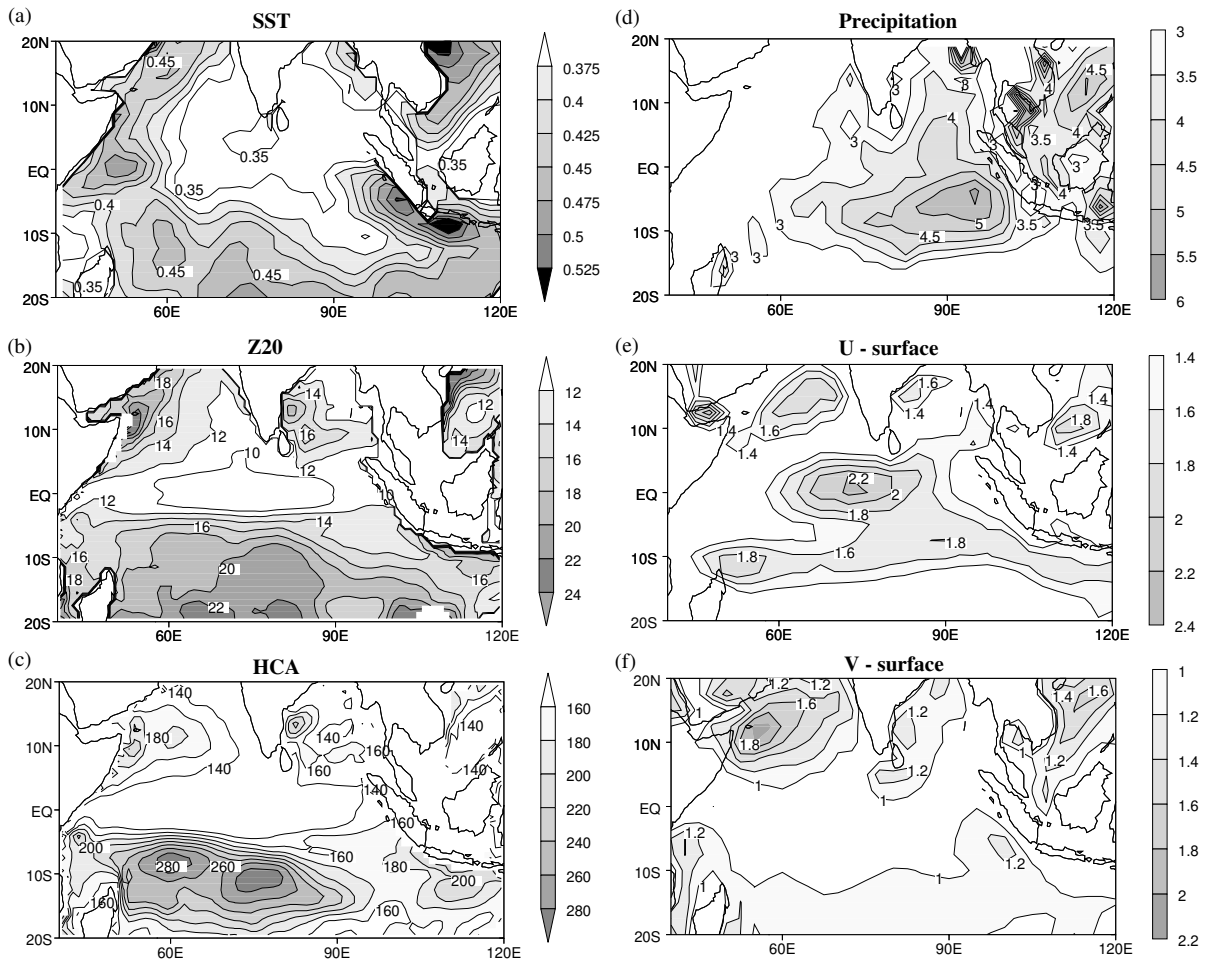

Fig. 1. RMS variance of (a) SST (°C), (b) Z20 (m), (c) HCA (°C m), (d) Precipitation (mm/day), (e) u-surface (m/s) and (f) v-surface (m/s).

thermocline variability on SST over the SWIO and a possible coupling of ocean Rossby waves there with the atmosphere. While Xie et al. (2002) indicate ENSO as the main forcing, Rao et al. (2002) suggest that the SWIO thermocline variability is largely due to the Indian Ocean Dipole (IOD). This difference in the statistics may be due to differences in the analysis period and reference indices used. The SST variability off Somalia (Fig. 1a) is largely due to variations in the intensity of the Somali wind (Schott, 1983; Rao et al., 1989; McCreary and Kundu, 1989; Fig. 1f). The latter is a major component of the Asian summer–monsoon system and its relationship to ENSO is well known (Lau and Nath, 2001).

Recent ocean modeling and observational studies have focused on the substantial SST anomalies off Sumatra/Java and in the equatorial western Indian Ocean (Reverdin et al., 1986; Murtugudde et al., 1998a, 2000; Murtugudde and Busalacchi, 1999; Behera et al., 1999; Webster et al., 1999; Saji et al., 1999; Yu and Rienecker, 1999, 2000). These SST anomalies appear to interact with atmospheric convection, equatorial zonal wind, and thermocline depth, much as Bjerknes suggested for Pacific ENSO. The zonal-asymmetric equatorial variability was originally called IOD, a terminology that emphasizes the role of east–west SST gradient in driving the equatorial zonal wind (Saji et al., 1999). Subsequent studies question this terminology, on the grounds that the western and eastern Indian Ocean SST anomalies are not significantly anticorrelated (Nicholls and Drosdowsky, 2001; Baquero-Bernal et al., 2002; Hastenrath, 2002). Some other studies refer to it as equatorial mode (Schott and McCreary, 2001). Le Blanc and Boulanger (2001) and Huang and Kinter (2002) find that while the cold SST anomalies off Java and Sumatra are a robust feature of all the Indian Ocean Zonal Mode (IOZM) events, the center of the warm SST anomalies in the western Indian Ocean varies significantly from event to event. We note that the terminology of this zonal interaction in the equatorial Indian Ocean is a subject of ongoing debate (Yamagata et al., 2002; Allan et al., 2001; Hastenrath, 2002), whose resolution is out of the scope of the present study but requires further

observational and modeling studies. In this paper, we use the term "IOZM", following US CLIVAR Asian-Australian Monsoon Research Prospects (2001), to avoid the possible implication of the term "dipole" for an anti-correlation between the western and eastern equatorial Indian Ocean.

In response to the SST variations during IOZM events, precipitation is reduced over the eastern equatorial Indian Ocean (EEIO), causing droughts on the eastern side of the basin throughout Indonesia, and engendering floods on the western side of the basin over parts of Africa (Birkett et al., 1999; Webster et al., 1999; Latif et al., 2000). In an earlier study, Hastenrath et al. (1993) noted the strong association between ENSO and zonal pressure gradient in the equatorial Indian Ocean during fall and that the attendant Indian-Ocean SST and wind anomalies are tied to the rainfall variations on the eastern African coast.

Murtugudde et al. (2000) utilized an ocean general circulation model (OGCM) to investigate the dynamics and thermodynamics of the IOZM, focusing on the 1997/98 event. They identified that the SST cooling off Sumatra and Java were mainly due to the unusually strong upwelling-favorable winds and entrainment cooling dominated the mixed-layer heat budget. By examining other IOZM events during 1958–97 from the OGCM simulation, they suggested that the IOZM is a natural mode of variability in the Indian Ocean–atmosphere interaction that can be triggered by ENSO.

On the other hand, the statistical study of Saji et al. (1999) suggests that IOZM events are largely independent of ENSO, but arise from air–sea coupled dynamics innate to the Indian Ocean. A coupled general circulation model corroborated this notion and simulated the IOZM that is independent of ENSO (Iizuka et al., 2000). The IOZM does not always occur in concert with El Niño (Reverdin et al., 1986; Meyers, 1996), and the relationship between the IOZM and ENSO is currently a matter of intense debate (Chambers et al., 1999; Iizuka et al., 2000; Nicholls and Drosdowsky, 2001; Allan et al. 2001; Baquero-Bernal et al., 2002; Xie et al., 2002; Krishnamurthy and Kirtman, 2002). All these studies reviewed above focus almost exclusively on the boreal

summer and fall, when the IOZM grows into finite amplitudes, but it remains unclear what triggers its growth in the first place and how this triggering takes place.

The present research examines the time evolution of the Indian Ocean climate system with a goal to understand how an IOZM event is initiated and what processes are involved. Distinct from previous studies, this paper focuses on the *boreal spring*, the season when the IOZM may be seeded albeit with small amplitudes. Potentially important processes to be examined include the following: external factors such as the Pacific Walker circulation and the Indonesian Throughflow (ITF), and variability internal to the Indian Ocean climate such as the alongshore upwelling-favorable winds off Sumatra due to variations in the monsoon convection. These three factors may not be mutually independent. Here we document the role of these factors in triggering the IOZM and offer a possible physical mechanism.

For this purpose, we use atmospheric and oceanic model-assimilated datasets over a common period (1950–99). Regarding some features for which there are insufficient observations, for example the ITF, we employ a realistic OGCM simulation. The first sign of a strong IOZM event is seen in March–April SST off south Java (Murtugudde et al., 2000; Xie et al., 2002; see also Fig. 3b), to which the ITF may contribute. Another important feature in the EEIO is an isothermal barrier layer beneath the mixed layer due to year-round deep convection (Sprintall and Tomczak, 1992). It prevents the wind-mixed layer from reaching the thermocline, thereby de-coupling the SST from the thermocline variability. We utlize the barrier layer thickness (BLT) estimated from the OGCM.

The main conclusion of the present study is that the Indian Ocean has a natural mode of coupled variability that is weak on its own, but intensifies in the boreal spring/early summer, often triggered by a developing El Niño or El Niño-like conditions in the tropical western Pacific. (Throughout this paper, seasons always refer to those in the Northern Hemisphere). Changes in the Pacific Walker circulation appear to be the main triggering mechanism. A series of sensitivity experiments

are conducted using the ECHAM5.1 atmospheric general circulation model (AGCM) to corroborate this remote forcing scenario.

2. Data

2.1. Observations/analysis

Sufficiently long atmosphere and ocean model assimilated analyses are available for the common period (1950–99), and they provide an opportunity to examine air–sea interaction in the Indian Ocean. The atmospheric data are adopted from the NCEP-NCAR renalyses products (Kalnay et al., 1996), and the oceanic variables stem from the Simple Ocean Data Assimilation (SODA) products of Carton et al. (2000). The SST is also adopted from NCEP-NCAR reanalyses products. SST from SODA or from the UK Hadley Centre for Climate Prediction product—GISST— essentially yields similar results. The atmospheric variables at standard pressure levels with horizontal resolution of $2.5 \times 2.5°$ are available. SODA has a resolution of about $1° \times 0.45°$ longitude–latitude resolution in the tropics, and has 20 vertical levels with 15 m resolution near the sea surface. The usefulness of SODA for studying the Indian Ocean coupled dynamics has been demonstrated in Xie et al. (2002). The $20°C$ isotherm, used to denote the depth of the thermocline (henceforth referred to as Z20), temperature at various depths, and heat content anomalies (HCA, heat stored in the upper 400 m), representative of sea-level changes, are the main variables taken from SODA. In addition, monthly mean precipitation from the CPC Merged Analysis of Precipitation (CMAP) product for the period 1979–2000 is adopted from Xie and Arkin (1996).

In the present study, the monthly mean climatology is first calculated for the study period and anomalies are simply departures from this climatology. Additionally through harmonic analysis, the decadal/inter-decadal components are discarded and the variability contained only at interannual time scales (16–84 months) is retained.

Due to the unique dynamical relationship between precipitation and the divergent component

of wind in the tropics, the latter is used to depict the three-dimensional mass flow associated with the Pacific Walker circulation. It is recognized that in the tropics the constraint of geostrophy on the divergent circulation is weak, and so there is considerable sensitivity to the diabatic heating field, particularly that associated with moist processes (Trenberth et al., 2000). In data-sparse regions, such as the Indian Ocean, the analyses will depend heavily on the first guess supplied by the forecast model; this in turn will be sensitive to the diabatic heating distribution produced by the physical parameterizations. Despite this constraint, the mean annual cycle of the divergent winds in the NCEP reanalyses, in terms of thermally direct circulations is realistic and in agreement with CMAP precipitation (Trenberth et al., 2000). As in the climatology (Trenberth et al., 2000), the anomalous divergent winds from the ECMWF Re-Analysis for the available period (1979–93) are in good agreement (not shown) with those of the NCEP/NCAR products. Therefore, we assume that the end results of our analysis are not expected to be significantly influenced by the assimilation procedure.

2.2. Ocean model output

We use the monthly estimates of ITF from a long integration (1950–99) of the OGCM of Murtugudde et al. (1996). The model is a reduced-gravity primitive equation model configured for the tropical Indian and Pacific Oceans. The model consists of 19 sigma-coordinate layers beneath a variable thickness surface mixed layer (Chen et al., 1994). The present simulation is forced by NCEP/NCAR reanalysis monthly winds for the period 1950–99. The ITF is estimated as the horizontally and vertically integrated transport in the top 400 m between northwest Australia and Java. The simulation of the seasonal cycle of the ITF, interannual variability and its impact on Indian Ocean climate has already been demonstrated in Murtugudde et al. (1998b). The BLT is defined as the difference between an isothermal layer defined as SST-0.5°C and the mixed layer as resolved by the model, consistent with Sprintall and Tomczak (1992). The advanced mixed-layer

scheme of Chen et al. (1994) combined with the sigma coordinate allows higher model resolution below the mixed layer with thickness of order 2 m. The model has active salinity and freshwater forcing is included as a natural boundary condition. Therefore, BLT is sensitive to model salinity in addition to temperature. The veracity of model BLT has been shown in Murtugudde and Busalacchi (1999).

Due to some constraints in SODA, we analyse the OGCM output for certain ocean variables. For example, in SODA the SST is restored and the salinity is relaxed to Levitus climatology. Therefore, a complete mixed-layer heat budget is not feasible (Section 4.2.2). Further, coarse resolution near the surface in SODA model means BLT cannot be approximated diagnostically. Our investigation (not shown) indicates a poor estimation of ITF in SODA, especially its seasonal cycle. On the other hand, the OGCM is forced with satellite-derived precipitation and a simple atmospheric boundary layer model derived evaporation, which better capture salinity, BLT and surface fluxes variation. We use ITF, BLT and mixed-layer heat budget terms from the OGCM. The spatial correlation between the depth of the thermocline from SODA and OGCM is very high in the EEIO (not shown). Therefore, our conclusions are not likely to be influenced by the OGCM variables. Similarly, since SODA has more reliable depth structure because of observational constraints, we use the 20°C isotherm, heat content anomalies, and temperature at various depths from SODA.

3. Air–sea interaction and seasonality

The thermocline feedback by which the subsurface fluctuations are communicated to the surface (SST) is a key process through which coupled dynamics grow and intensify. The resulting surface temperature fluctuations modify atmospheric convection that subsequently influences the atmospheric circulation. The changing winds force changes in ocean currents and thermocline depth, completing the cycle of Z20→SST→Precip→Winds→Z20, as in ENSO (Bjerknes, 1969). Unlike

heat content, Z20 is not affected by SST and therefore represents the subsurface variability better.

3.1. Interannual variability

Fig. 1 shows the rms variance of key physical quantities involved in the Bjerknes feedback loop. In agreement with previous studies, variations at the surface (SST) and in the subsurface in the equatorial central and over most of the Indian Ocean are small. Regions of large variance are the upwelling zones off Somalia and off Java–Sumatra, as well as in the SWIO (8–18°S, 50–85°E) where the correlation between Z20 and SSTA are significant (Fig. 2). Over the SWIO, where the thermocline is closer to the surface in the mean, the influence of thermocline variations on SST is
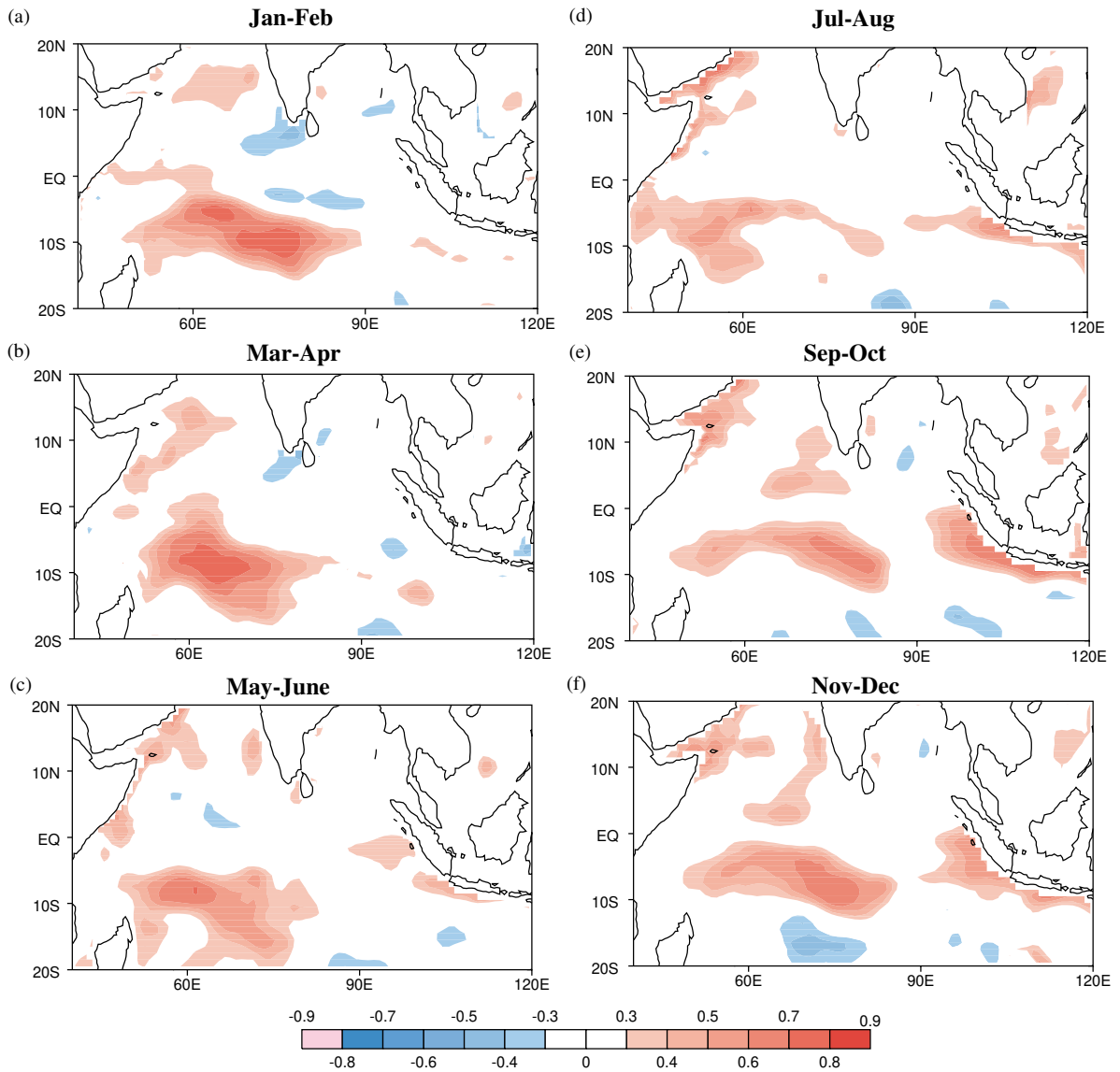

Fig. 2. B-monthly correlation between SST and Z20. Values significant at 95% levels are shown.
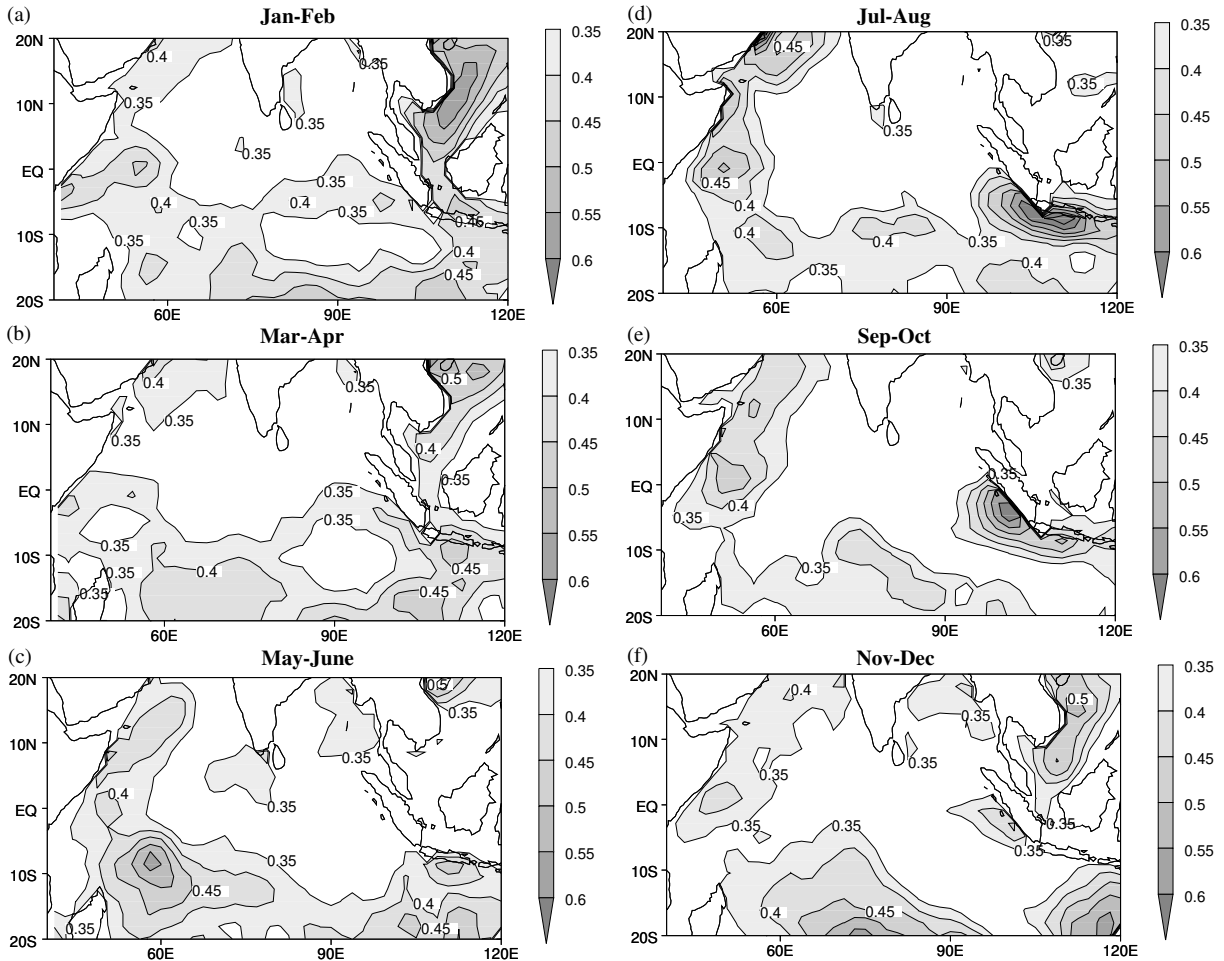
Fig. 3. RMS variance of bi-monthly SST in °C. The contour interval is 0.05 and values greater than 0.35°C are shaded progressively.

strong during December–May (Fig. 2). Apart from local Ekman forcing (Murtugudde and Busalacchi, 1999), the thermocline and SST over SWIO are influenced by oceanic Rossby waves, having maximum impact during December–May (Xie et al., 2002). While there is evidence for two-way coupling both in the EEIO and SWIO, the present research focuses on the life cycle of the former. In the present study, EEIO refers to the area averaged over (10°S–Eq, 90–110°E).

For the available period, the precipitation variability over the EEIO (>5 mm/day) is larger than over most of the monsoon domain (Fig. 1d). In the equatorial central Indian Ocean (60–90°E), the zonal wind variability (∼2.5 m/s) is as strong

as the mean (Schott and McCreary, 2001). In this region, equatorial winds have direct impact on ocean currents and the ITF by forcing equatorial and subsequently coastal waves (Murtugudde et al., 2000; Sprintall et al., 2000).

The SST variability is strongly phase-locked to the annual cycle (Fig. 3) and so is its relationship with Z20 (Figs. 2a–f). More importantly, in the EEIO, we recognize that spring/early summer is the 'transitional time' when the thermocline begins to influence the SST. In this region, the first signature of SST variability (∼0.45°C) is evident off Java in March–April (Fig. 3b), which is apparently unrelated to thermocline changes (Fig. 2b). From May onwards (Fig. 2c), the

thermocline perturbations start to influence SST off Java, thus setting the stage for coupled dynamics to grow. This localized SST variability intensifies (May–June), and extends north-west-wards off Sumatra in July–August (Fig. 3d) during the established phase of the Asian Summer Monsoon. During September–October, the SST and its relationship with Z20 peak off the Sumatra coast (Fig. 2e). In the EEIO, the influence of Z20 on the SST weakens in November–December and ceases thereafter. The life cycle in the relationship between thermocline and SST in the EEIO (Fig. 2) is consistent with the rms SST evolution in Fig. 3. The phase-locking nature to the annual cycle warrants the examination of the role of the background state (annual cycle) on the evolution of the IOZM (Section 3.3).

3.2. Natural mode of coupled variability in the Indian Ocean

From observations/analyses, there is no unique method to identify 'modes of coupled variability'. We turn to simple diagnostics that consider all the essential variables that are important for air–sea interaction to identify weak or strong IOZM years.

We examine the evolution of anomalous SST in concert with Z20 and alongshore winds averaged over $10°$S-Eq, 90–$110°$E. In addition, the evolution of zonal wind anomalies over the equatorial Indian Ocean ($5°$S–$5°$N, 60–$90°$E) is taken into account. The rms variance of the ocean–atmosphere variables (Fig. 1) is relatively high in these regions and collectively reflect a Bjerknes-type mechanism.

Based on statistics in Figs. 1–3, a strong IOZM year is defined to be any given year when all the following four quantities co-exist: negative SSTA, shallower than normal Z20, stronger than normal south-easterlies over the EEIO, and anomalous easterlies over the equatorial central Indian Ocean, for a period of 5–6 months and individually exceeding a threshold of 1.0 s.t.d. Based on this criteria in the period of analysis (1950–99), six strong IOZM years are identified. The other two categories identified are aborted (14 years) and weak (7 years) IOZM years. The aborted years are those when a signal for IOZM appears in spring

but switches sign abruptly thereafter (Fig. 4a). The years when the above anomalies are greater than zero but less than one standard deviation are recognized as weak IOZM years (Fig. 4c). For brevity, only the characteristics of SSTA, the variable that has direct impact on the atmosphere, are shown (Fig. 4). The mean evolution, obtained by averaging all the events in the individual category, also is shown in Fig. 4. It is to be noted that for the available period (1979–99) the
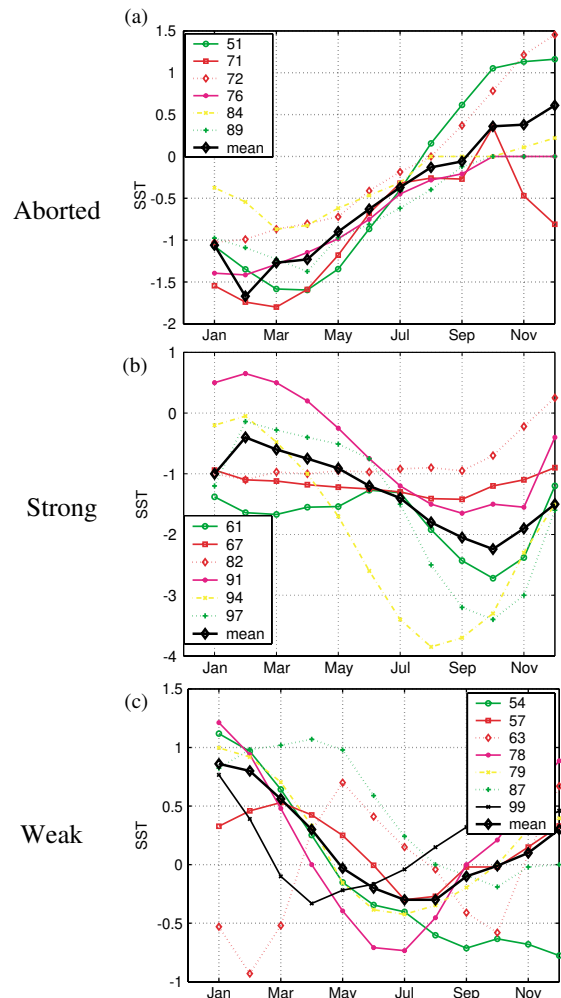

Fig. 4. Time evolution of standardized SST anomalies in the EEIO (90–$110°$E, $10°$S–Eq) for: (a) aborted, (b) strong and (c) weak IOZM years. The monthly s.t.d. of SST is $0.3°$C. The mean evolution obtained by averaging all the events in the individual category is also shown.

precipitation anomalies are in-phase with SST and other variables.

As an example, Fig. 4(a) shows six aborted events when SSTA reaches a minimum (1.0–1.5 s.t.d) in March–April but change sign (or warm up) thereafter. Unlike other studies (e.g., Saji et al., 1999), Fig. 4(a) reveals that the EEIO cooling in 1972 falls into the aborted category. A closer scrutiny of spatial patterns of SSTA (not shown) divulge that in 1972, the WIO was anomalously warm while EEIO was near normal, except for moderate cooling off Java. In addition, the upwelling-favorable alongshore winds and Z20 do not meet the objective criteria, except off Java (8°S, 105–108°E) during September–December of that year, a common feature of all El Niño years (Krishnamurthy and Kirtman, 2002). Both COADS and Reynolds SST products indicate that the intensity of the IOZM event in 1963 is weak. Therefore, the year 1963 has been treated as a weak IOZM year (Fig. 4c).

Only in 3 years (1961, 1994 and 1997) does the EEIO SSTA exceed 2.0 s.t.d. (Fig. 4(b)), while in other 3 years it lies within 1.0–2.0 s.t.d (1967, 1982 and 1991). In terms of absolute magnitude, these six events are classified as strong, although the growth in some years (e.g. 1967 or 1982) is slow compared to 1994 or 1997. These 6 years are all accompanied with anomalous Ekman divergence over the EEIO (F. Schott, 2001, personal communication). The XBT measurements along a section from Australia to Java captures upwelling and shallowing of thermocline during 1991 (Feng et al., 2001). Like in the evolution of individual El Niño events (e.g., Fedorov and Philander, 2001), there is inter-event dispersion in the evolution of IOZM events also. Consistent with the rms variance noted in the EEIO (Fig. 3), in strong years there is a tendency for the SSTA to grow and peak in summer and fall, respectively.

Fig. 5a shows the standardized monthly Southern Oscillation Index (SOI) for the six strong IOZM years. A 3-month running mean was applied to the raw SOI before producing Fig. 5a. Except for the event in 1967, when the SOI is only marginally negative for a short period in May, in the other 5 years there is a tendency for the SOI to become significantly negative during spring/early
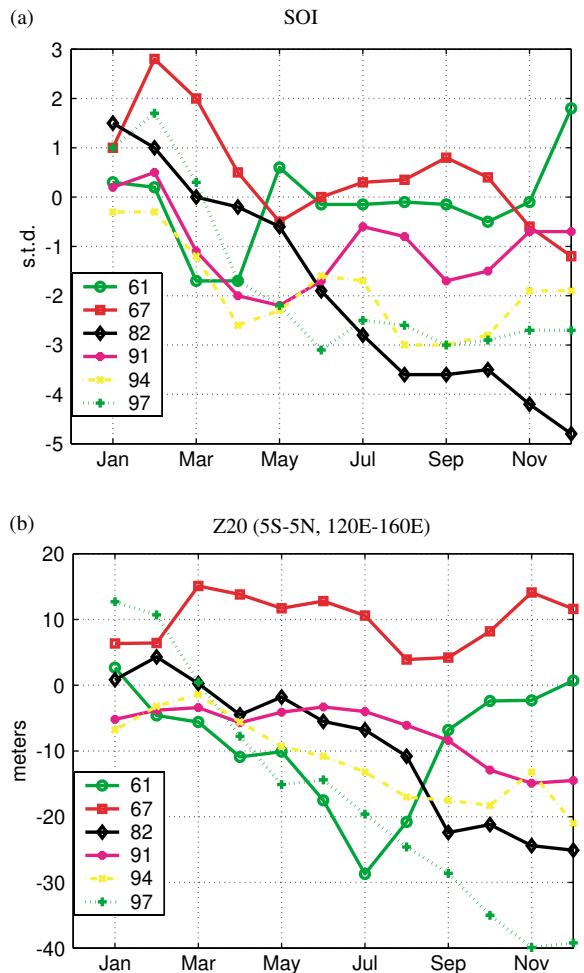

Fig. 5. Monthly evolution of (a) Southern Oscillation Index (SOI) in units of standard deviation and (b) anomalous thermocline depth (m) averaged in the equatorial western Pacific (5°S–5°N, 120–160°E) during all strong IOZM years.

summer. Allan et al. (2001) also reported that the dipole SST index defined by Saji et al. (1999) is significantly correlated with SOI. Fig. 5b shows the anomalous thermocline depth averaged over the Indonesian Seas and equatorial west Pacific (5–5°S, 120–160°E). Consistent with SOI, the tendency of shallower than normal Z20 during spring/early summer is again indicative of warm ENSO conditions in the regions of South Java–Indonesian seas (Meyers, 1996) and in the western Pacific (Flohn, 1987). Both from SOI and Z20, it is found that most of the El Niño-like conditions

observed in spring continue to grow and the thermocline sholas in winter with an exception in 1961. The SOI tends to be negative for a short period in the spring of 1967 when Z20 in the western Pacific also shoals, albeit La Niña conditions prevailed in the eastern Pacific later in fall/winter. As corroborated by Flohn (1987), Meyers (1996) and Kapala et al. (1994), both from atmospheric and oceanic parameters and therefore in the coupled system, El Niño-like conditions exist in the west Pacific, at least in spring/early summer in 1961 and 1994.

Based on SST anomalies off Peru, Deser and Wallace (1987) note lack of relationship between El Niño and above normal Darwin pressure anomalies for few years. The authors, however, conclude that in these years, the equatorial central Pacific (NINO3.4 region) SST and rainfall were above normal and also note below normal sea-level pressure at Tahiti. Based on Reynolds SST, with the exception of 1967, during spring/early summer of other strong IOZM years, positive SST anomalies prevail in the NINO 3.4 region (not shown). Therefore, the SOI tendency we note in Fig. 5a are largely influenced by El Niño-like conditions.

Fig. 4c shows that in weak IOZM years, the SST cooling in the EEIO is < 1.0 s.t.d but has a similar life cycle to those of strong IOZM events. These weak events tend to peak in July-September, 2–3 months earlier than the strong events. Fig. 6 shows the monthly evolution of depth-temperature profile off South Java for weak years. It is clear that the thermocline does not rise enough to influence the SST, implying that thermodynamic air–sea interaction prevails during weak years.

The inference from Figs. 4b, 4c, 5a, 5b and 6 is that there is a natural mode of coupled variability in the Indian Ocean that is weak on its own, as suggested by Latif and Barnett (1995), but intensifies due to external forcings. Strong events tend to occur with El Niño-like conditions, when the contribution by the ocean dynamics to SST cooling is substantial (Behera et al., 1999; Murtugudde et al., 2000). Another impression from all the panels in Fig. 4 is that weak or aborted events are clustered in the 1950s, 1970s and 1980s, while strong events are more prominent in the 1960s and 1990s. Therefore, even if El Niño-like conditions prevail in other years, the nonoccurrence of strong IOZM is possibly asso-

ciated with the lack of thermocline influence and/or preconditioning of the ocean in the EEIO.

3.3. Annual cycle over the EEIO

Fig. 2 illustrates that during early summer (fall) the thermocline influence on SST begins that eventually leads to the growth (peak) of the IOZM. The phase locking nature of IOZM demands that the annual cycle of key ocean–atmosphere variables in the EEIO (Fig. 7) be examined. The ITF transport estimates in Fig. 7d are from geostrophic calculations of Meyers (1996) based on repeated XBT line along a section from Australia to Java. The ITF is measured as a westward current and therefore negative values imply strengthened ITF. The annual range of SST, Z20, OLR, ITF and BLT are $1.5°C$, $25\,m$, $20\,W/m^2$, $10\,Sv$ and $14\,m$, respectively. Even over the equatorial region, the annual harmonic dominates in SST and OLR, while the semi-annual part is prevalent in Z20, ITF and BLT. The BLT is sensitive to both freshwater input from rainfall and entrainment due to ocean dynamics (Masson et al., 2002). It is evident from Figs. 7a and b that the EEIO is a warm pool region (SST $> 27.5°C$) all year round where deep convection (OLR $< 240\,W/m^2$) co-exists. Peculiarily, the annual cycle of SST is out of phase with convection: the strongest convection (OLR $< 220\,W/m^2$) occurs in September when SST is at its minimum.

The concurrent annual minimum in convection, BLT, thermocline depth and ITF during spring implies that there is a 'time window' in the annual cycle during which the ocean–atmosphere system in the EEIO is possibly susceptible to external forcings for interannual anomalies to grow. Thus, the seasonality in the background state may be essential for the development of IOZM, like that for El Niño in the Pacific (e.g., Xie, 1995). This hypothetical picture needs validation with careful numerical experiments using coupled models.

4. Anomalous walker circulation and the IOZM

In the correlation statistics and composite figures presented in this and following sections,
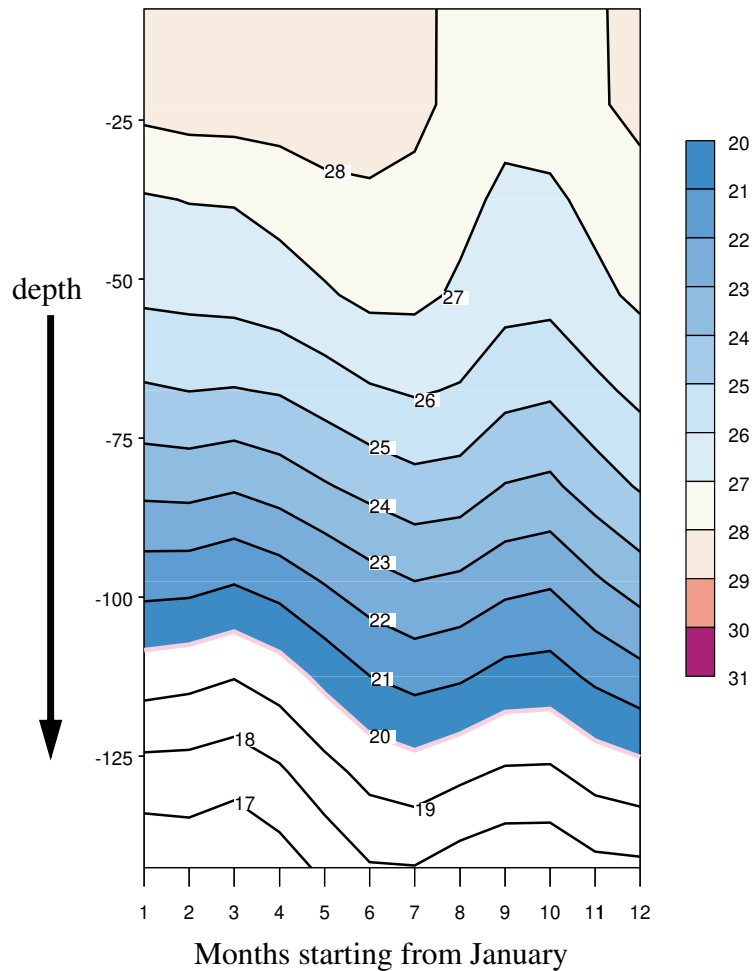
Fig. 6. Monthly evolution of depth (in m) versus temperature off South Java for weak IOZM events. The depth of the thermocline indicated the 20°C isotherm is shown in pink and values greater than 20°C are shown in color.

only statistically significant values (95% level) and regions are shown and discussed. For the spatial correlation fields grid point *t*-test is applied. The precipitation composites are made only with the years for which observations are available.

4.1. EEIO spring conditions

Fig. 8a (Fig. 8b) shows composites of anomalous surface winds and Z20 during spring for the weak (strong) IOZM years. The composite monthly evolution of anomalous BLT (precipitation) averaged over the EEIO for weak and strong IOZM years are shown in Fig. 9a (Fig. 9b). During

weak years, the equatorial easterly anomalies force upwelling equatorial and coastal Kelvin waves leading to shallower than normal Z20 (Fig. 8a). However, a signature of above normal precipitation and BLT (Fig. 9) associated with weaker than normal alongshore upwelling-favorable winds off Java (Fig. 8a) is evident, precluding the development of the IOZM. Even a 2 m changes in the BLT will prevent wind mixing from entraining thermocline waters into the mixed layer. By contrast, in strong years, alongshore winds are enhanced off Java where SST variance reaches a local maximum during this time of the year (Figs. 3b and c). Moreover, precipitation and subsequently the
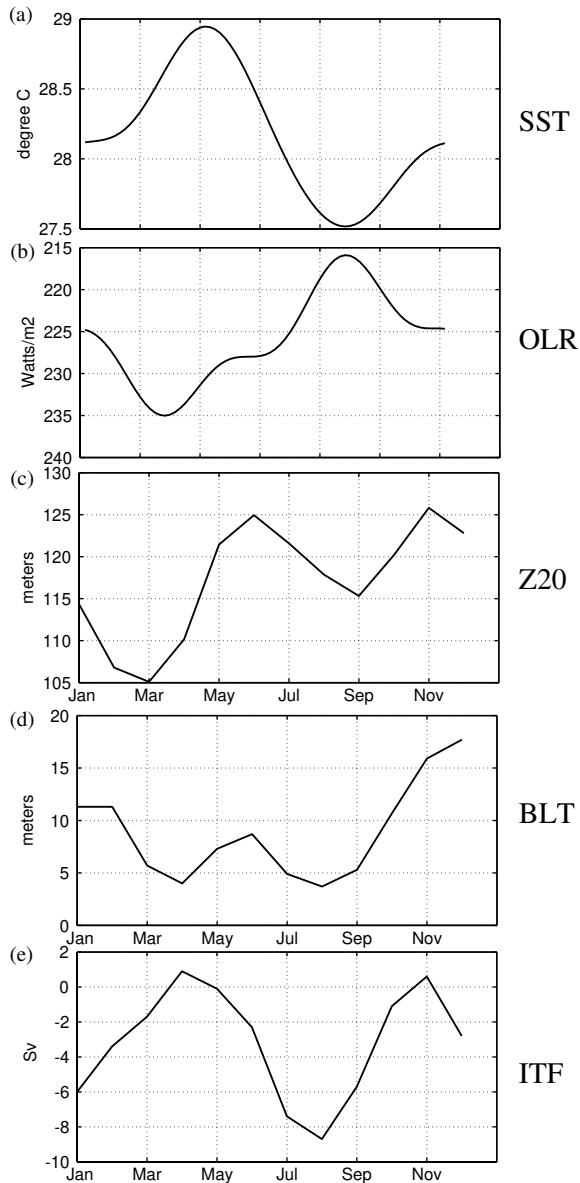
Fig. 7. Annual cycle of (a) SST, (b) OLR, (c) thermocline depth (Z20), (d) barrier layer thickness (BLT), averaged over the EEIO (90–110°E, 10°S,Eq) and (e) Indonesian Throughflow (ITF).

BLT are continually reduced from spring onwards, and they both peak during fall. The broad agreement between the composites of precipitation and BLT enhances the confidence in using the OGCM output in the present study. Once the BLT

is reduced in spring, upwelling becomes more effective in cooling the SST because cooler water is entrained into the mixed layer (Murtugudde et al., 2000). The contrasting features in Figs. 8 and 9 leave us with some pertinent issues to understand in the EEIO during spring: What are the possible processes that are responsible for (a) the reduction in precipitation and erosion of BLT, and (b) the enhancement of alongshore winds that are noted in strong IOZM years?

From simple diagnostics we show that the atmospheric variations in the equatorial Indian Ocean during spring are remotely controlled. During March–April, the intense climatological precipitation associated with the ITCZ in the Indian Ocean lies around the EEIO-maritime continent (Fig. 10a), with a local rms variance of about 1.0 mm/day (not shown). To represent the ITCZ fluctuations in spring, we define a precipitation index by averaging the precipitation anomalies over the region 90–120°E, 10°S–Eq. We now explore what controls rainfall variations in this key region to the initiation of the IOZM. The simultaneous correlation in spring between this ITCZ index and SSTA (Fig. 10b) reveals the western-central Pacific (150°E–150°W) as the only significantly correlated region in the equatorial band. The Indian Ocean ITCZ during spring is not correlated with SSTA either locally or in the eastern Pacific. Therefore, both in the annual cycle (Fig. 7) and at interannual timescales, the precipition in the EEIO during spring is unrelated to local SST, a key finding of the present study. The ITCZ-SST correlation pattern evolves with the seasons; in fall, the ITCZ index is very highly correlated with both local and eastern Pacific SSTA (Fig. 11), in sharp contrast to the distribution in spring. In general, some previous studies (e.g. Graham and Barnett, 1987) have shown the SST-convection relationship breaks down in the warm pool. Our contribution is the demonstration that in the specific region of EEIO, and in specific season of boreal spring, the local SST-convection breaks down (but returns in fall) and that the EEIO convective anomalies are remotely forced by equatorial western-central Pacific SSTA. We are unaware of any studies that make these two points, and particularly the seasonal dependency
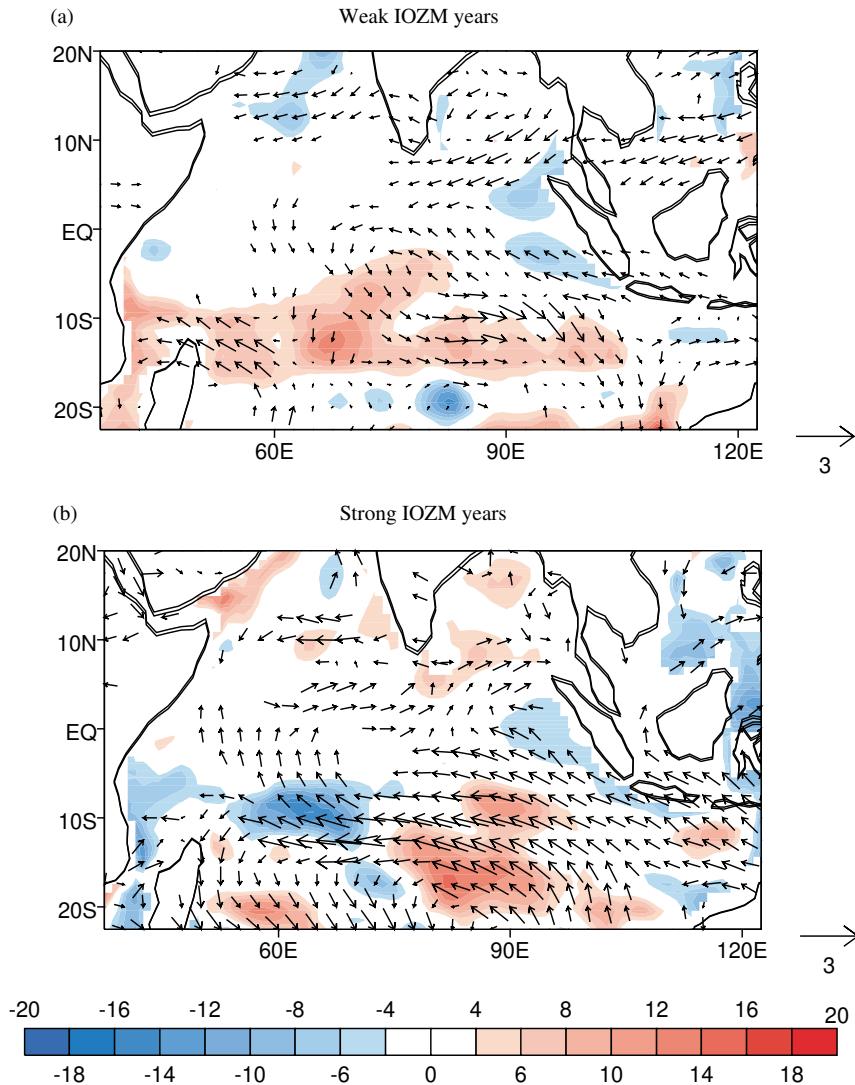
Fig. 8. Boreal Spring (MAM) composites of anomalous surface winds (m/s) and thermocline depth (m, shown in colour) for: (a) weak and (b) strong IOZM years. Values significant at 95% level are only shown. The reference wind vector (m/s) is also shown.

between SST and convection in the EEIO is not addressed in previous studies. To understand the nature of this external control, we examine the relationship between precipitation and divergent and rotational components of the winds from NCEP/NCAR reanalyses.

The spring anomalous precipitation composites from CMAP for the strong IOZM years (Fig. 12a) show enhanced precipitation in the near-equatorial western Pacific, subsequently leading to modulations

to the thermally direct circulation. To extract the east–west overturning divergent circulations, we follow the methodology proposed in Trenberth et al. (2000). The anomalous mass flux associated with the u-component of the divergent wind and vertical velocity at all pressure levels are computed first (details in Trenberth et al., 2000). A composite vector plot of the mass flux averaged meridionally over 10°N–10°S and for spring season in strong IOZM years is shown in Fig. 12b. The composite

(a)

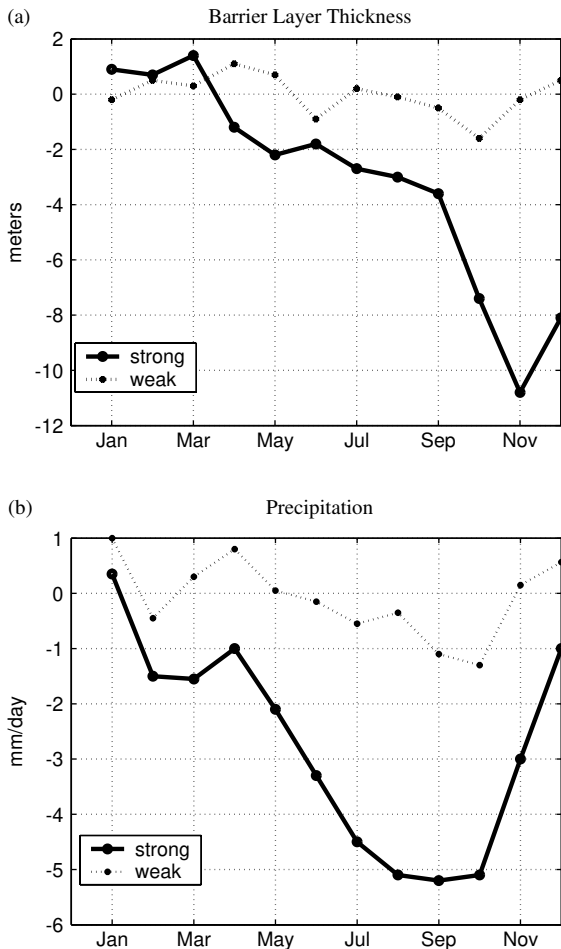Barrier Layer Thickness

(b)

Precipitation

Fig. 9. Strong and weak IOZO years composite evolution of anomalous (a) barrier layer thickness (m) and (b) precipitation (mm/day) averaged over the eastern equatorial Indian Ocean (90–110°E, 10°S–Eq).

circulation indicates that the ascending air over the western-central Pacific descends over the EEIO-maritime continent. This anomalous subsidence results in negative precipitation anomalies in the EEIO (Fig. 12a). This result, in agreement with Fig. 10a, confirms that the precipitation anomalies are indeed due to the intensity of the anomalous subsidence rather than due to local SSTA. It is well known that in the warm-pool regions, such as the EEIO, persistent surface divergence due to remote forcing changes the stability of the moist atmosphere, thereby suppressing the convection even when the total SSTs are above 28°C (Graham and

Barnett, 1987; Webster et al., 1998). The SST during March–May in the EEIO attains its annual maximum of 29°C (Fig. 7a), and therefore some external forcing is necessary to reduce the convection and subsequently reduce BLT for dynamic air–sea interaction to develop.

4.2. How is an IOZM triggered?

4.2.1. Atmospheric processes

The time mean negative precipitation anomalies lead to a local heat sink in the EEIO. To extract the atmospheric response forced by this heat sink, we regress the precipitation (ITCZ) index onto the surface winds for March–April. As expected from linear theory (Matsuno, 1966; Webster, 1972; Gill, 1980), an anticyclone develops as a Rossby-wave response in the southeastern Indian Ocean (Fig. 12a). The positioning of the center of the anticyclone, roughly 20° to the southwest of the center of the heat sink, confirms the linear response. Climatologically, the alongshore winds off Java are noticeable from mid-March (e.g. Schott and McCreary, 2001). The anomalous anticyclone therefore will, enhance the upwelling-favorable winds at the coast, cooling the SST through both latent cooling and upwelling processes (Fig. 13, discussed later). The twin cyclones straddling the equatorial western-central Pacific are also Rossby-wave responses to enhanced precipitation there (Fig. 12a), an indicator of the developing phase of El Niño (Wang and Weisberg, 2000). Even in the spring of 1961 there is a tendency for SOI to weaken which did not amplify later in summer or fall. Thus, it is reasonable to argue that El Niño-like conditions by inducing anomalous subsidence in the EEIO can trigger an IOZM event. Gualdi et al. (2003) analyse the output from a long intergration of a coupled GCM and note a strong correlation between the anomalous mean sea-level pressure in the southeast Indian Ocean and NINO3 SSTA. Based on this, they suggest that during its developing phase, El Niño could create conditions for the initiation of the IOZM. The changes in the mean sea-level pressure in their study reflect the cyclonic or anticyclonic circulation anomalies, we identify in Fig. 12a. The robustness in the results from a completely
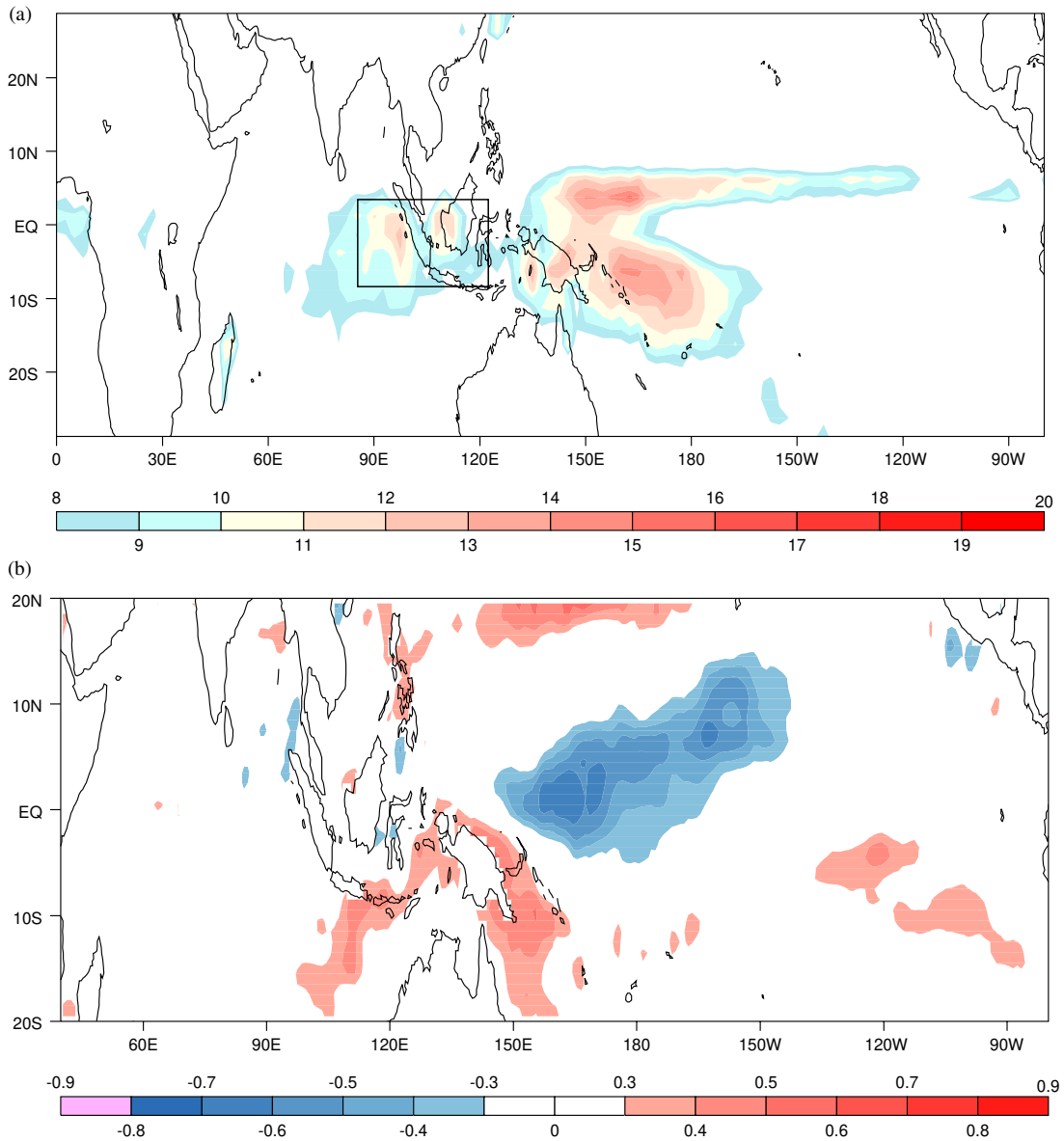
Fig. 10. (a) Boreal spring precipitation climatology and values greater than 8 mm/day are only shown. The region representing the Indian Ocean ITCZ (90–120°E, 10°S–Eq) is shown as rectangular box, (b) simultaneous correlation between March–April ITCZ index and SSTA for the period 1979–2000. Correlations significant at 95% level are only shown.

different source enhances the confidence in our diagnostics.

4.2.2. Oceanic processes

A possible caveat is once the precipitation is suppressed and anomalous subsidence is strength-ened in the EEIO, enhanced radiative flux will tend to warm the SST and shallow the mixed layer, increasing the stratification and suppressing sur-face cooling. As shown from the composites of BLT (Fig. 9a), there is no indication for the deepening of the BLT during this period, and
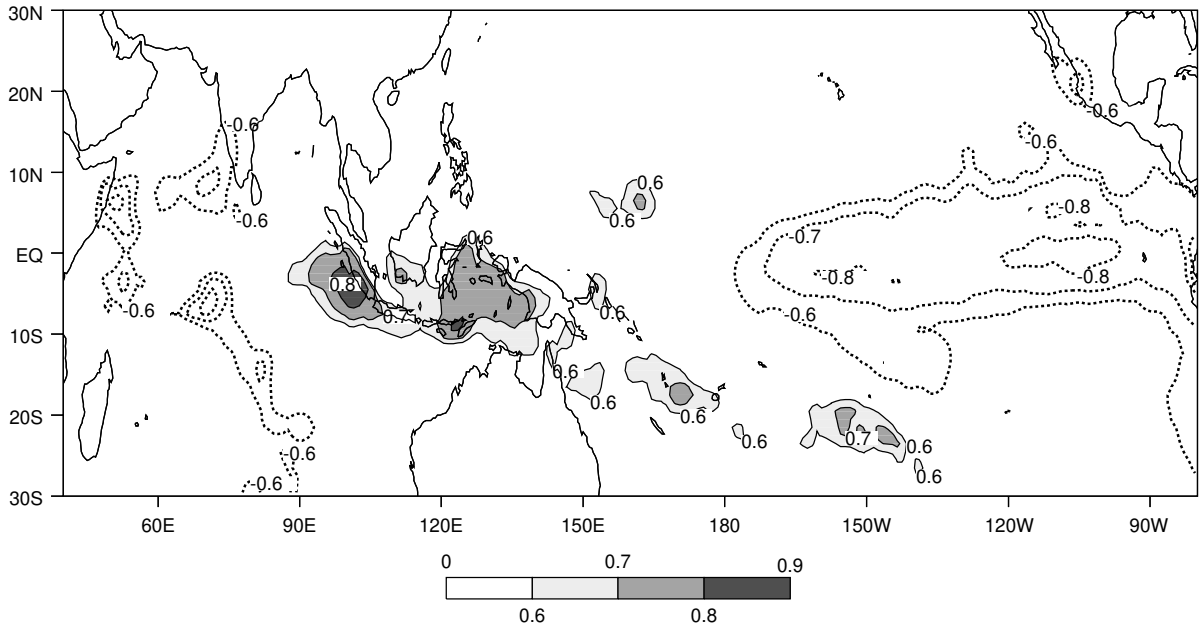
Fig. 11. Simultaneous correlation between Indian Ocean ITCZ, precipitation averaged over (10°S–Eq, 90°E–120#) with SSTA for the fall (September–November) season, estimated for the period 1979–2000. Correlations greater than 0.6 are shown. Positive values are shaded progressively and negative values are shown in contours.

oceanic processes clearly dominate the SST cooling aided by the enhanced evaporative cooling. An investigation (not shown) to the OGCM's mixed-layer depth, heat and salinity fluxes indicate an initial deepening of mixed-layer depth off Java in March–April, possibly due to increase in salinity, but from May onwards, the mixed-layer depth begins to shallow. The enhanced upwelling reduces the BLT and shallow the mixed layer too, overcoming the effects due to heat fluxes. Consistent with our results, Masson et al. (2002) showed the role of salinity and ocean dynamics in the BLT in the EEIO.

To identify the causes for cooling of SST during spring/early summer, we examined areal average of the anomalous terms in the mixed-layer temperature equation in the OGCM. The temperature tendency equation and processes that determine SSTA are described in Murtugudde et al. (2000). A composite evolution of the processes, obtained by averaging all the strong IOZM years is shown in Fig. 13. During spring/early summer in the coastal upwelling region off south Java

(95–105°E, 10–5°S), cooling is caused by entrainment and zonal advection terms. The meridional advection term's contribution becomes significant from June onwards. The latent flux also contributes to SST cooling by evaporation due to anomalous winds (latent cooling) till July. The collective cooling of SST by the various processes lead to initiating IOZM event off south Java. It should be noted here that the SST variance off south Java peaks in July August (Fig. 3) consistent with the rate of change in mixed-layer temperature presented in Fig. 13. It also should be pointed out here that climatological radiation is used in the ocean model simulation (Section 2.2). Given the fact that the model simulates the observed SST variability reasonably well, net downward heat flux is dominated by evaporative cooling during spring/early summer inspite of reduced precipitation and increased insolation. This feature is confmed for the ISCCP period (1983–94) when the interannual radiative flux anomalies are used in the model simulation (not reported here).

(a)   Precipitation

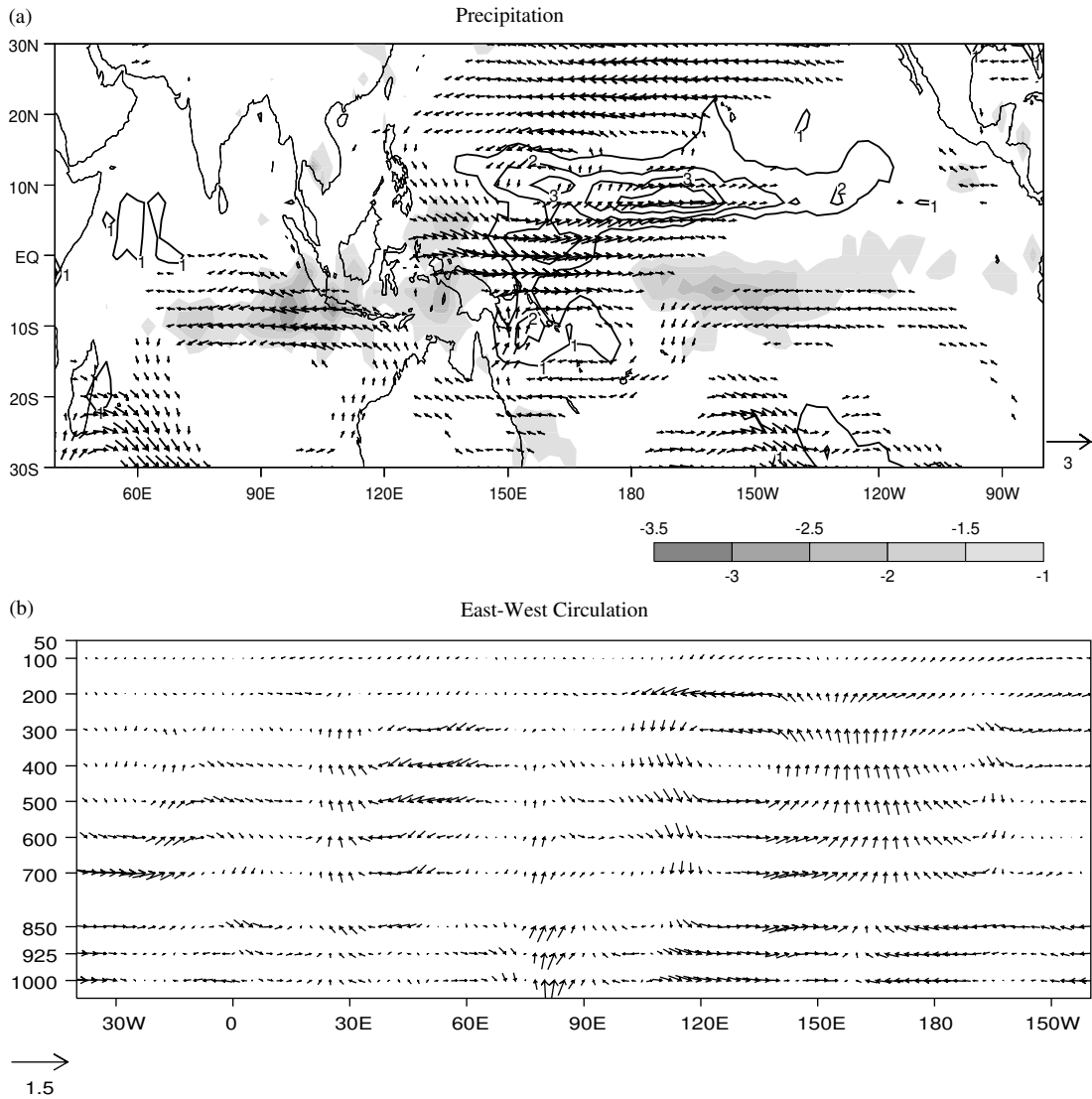(b)   East-West Circulation

Fig. 12. (a) Spring (MAM) composites of anomalous precipitation for strong IOZM years. The negative values in (a) are shaded progressively with an interval of 0.5 mm/day, while positive values are shown in contours with an interval of 1 mm/day. The precipitation index averaged over (90–120°E, 10°S–Eq) and for MAM, representing the Indian Ocean ITCZ, is regressed onto the surface winds and the statistically significant winds are shown in the top panel. The reference wind vector (m/s) is shown at the right bottom. (b) MAM composite of anomalous divergent east–west mass circulation constructed from the zonal component of the divergent wind and vertical velocity at each pressure level. The reference vector indicates the mass flux in kg/m^{2}s The methodology is explained in detail in Trenberth et al. (2000).

4.3. AGCM sensitivity experiments

To test the correlation statistics shown in Fig. 10b and the composites of Fig. 12, we carried out sensitivity experiments using the ECHAM5.1 AGCM. It is a global spectral model at T42 resolution and with 19 sigma levels in the vertical. The nonlinear terms and the parameterized
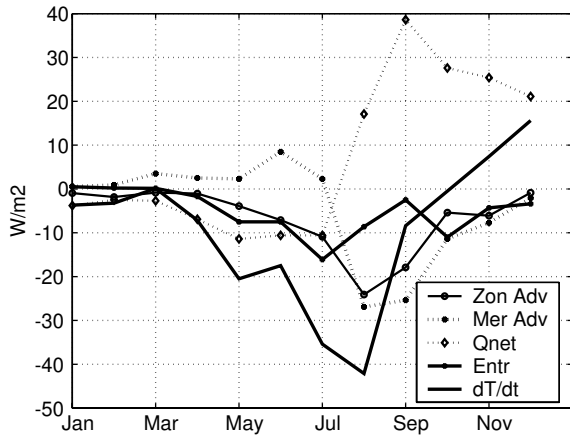
Fig. 13. Strong IOZM years composite evolution of anomalous zonal and meridional advection, net heat flux and entrainment for the ocean model mixed layer off south Java (95–105°E, 10–5°S), where IOZM is initiated. The sum of these terms is representative of rate of change of mixed layer temperature (dT/dt) and is also shown. During spring and early summer, entrainment and zonal advection contribute to cooling; Qnet (primarily latent heat) also contributes to the cooling.

physical processes are calculated on a 128×64 Gaussian grid, which yields a horizontal resolution of about $2.8° \times 2.8°$. The model details are described in Roeckner et al. (2001). Two sets of experiments are carried out. In the control experiment the AGCM is forced with monthly climatological SST and sea ice for 7 years, and the mean of the last 6 years is taken as the model climatology. Then, the response of the model atmosphere to EEIO precipitation variations to SST anomalies based on significant correlations in Fig. 10b are tested. In this run SSTA over the equatorial western-central Pacific (10°S–10°N, 150°E–150°W) are imposed. For this sensitivity experiment, the SST anomalies from January to December are obtained by compositing the six strong IOZM events and the model is run for 1 year starting from 1 January. To circumvent the atmospheric noise, a five-member ensemble approach, with changes only in the initial condidtions (1–5 January) but preserving the same SST forcing, are conducted.
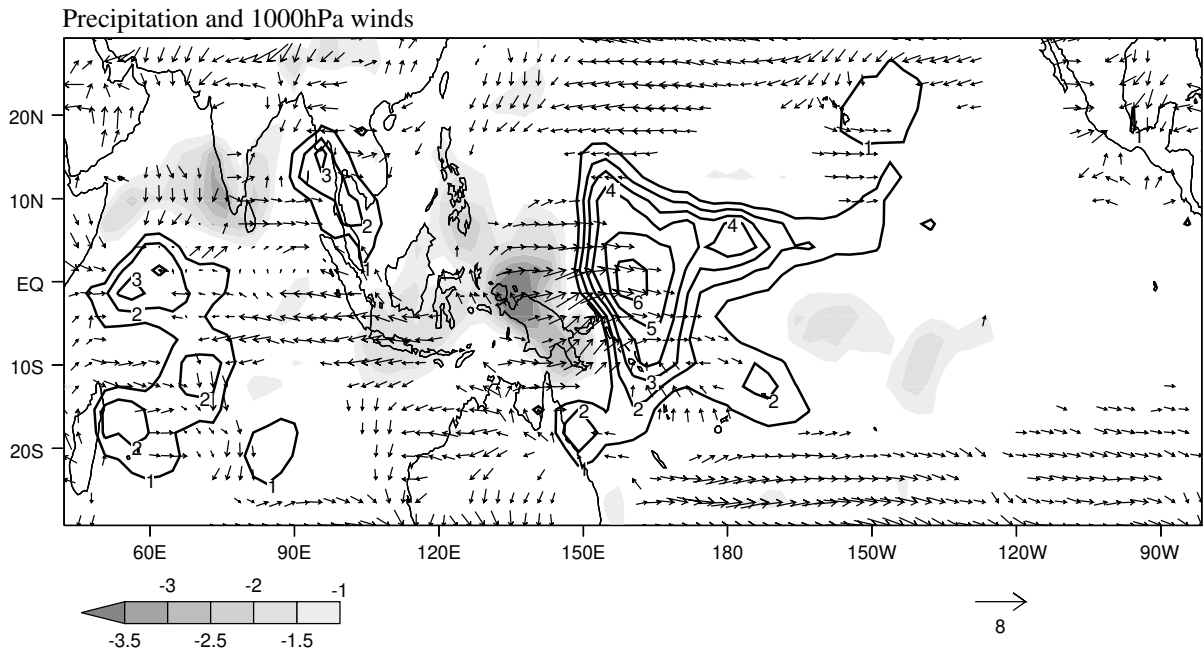

Fig. 14. Spring (MAM) ensemble mean precipitation and 1000 hPa wind anomalies from the AGCM simulation forced by SSTA over the equatorial western-central Pacific (10°S–10°N, 150°E–150°W). The negative precipitation values are shaded progressively with an interval of 0.5 mm/day while positive values are shown in contours with an interval of 1 mm/day. The reference wind vector (m/s) is shown at the right bottom.

Fig. 14 shows anomalous precipitation and 1000 hPa winds obtained from the sensitivity experiment. The anomalies are with respect to the model climatology. The enhanced precipitation due to the underlying warm SSTA in the equatorial western-central Pacific are readily captured. It should be noted here that no SST anomalies are imposed in the EEIO/maritime continent sector, yet significant negative precipitation anomalies, associated with low-level divergence are noted. The anomalous winds converge in the equatorial western Indian Ocean, resulting in positive precipitation anomalies there, much as in observations (Fig. 12a). The perturbations to the Pacific Walker circulation induced by Pacific SST anomalies cause the negative precipitation anomalies in the EEIO/maritime continent. Forced by this heat sink, upwelling-favorable winds are enhanced in the southeastern Indian Ocean. Therefore, the sensitivity experiments with the AGCM support our hypothesis that external forcing (Pacific) leads to anomalous upwelling-favorable winds off Java and trigger an IOZM. There is, however, some disagreement in the AGCM results (Fig. 14) compared to observations (Fig. 12a), outside the region of our interest. Additional experiments with EEIO SST anomalies alone simulated very weak precipitation anomalies. Forced by this weak heat sink, low-level anticyclone in the southeastern Indian Ocean is weak indeed (not shown).

4.4. Some limitations

Albeit this confirmation from AGCM sensitivity experiments, there are some caveats in the statistics shown in Figs. 10 and 12. First, precipitation data are available only from 1979, which prevents us from studying the 1961 and 1967 strong IOZM years. Second, the relationship between the SOI and NINO3 SSTA is not perfect as in the case of 1994 (e.g., Soman and Slingo, 1997) but, as mentioned earlier, SSTA in NINO3.4 region indicates El Niño (Trenberth, 1997) and, the year 1994 has been considered as moderate or weak El Niño in many studies (e.g., Trenberth, 1997; Schott and McCreary, 2001). The important point is that, during spring, the SST gradient along the

equatorial Pacific is very weak, and therefore the regions of even small warm SST anomalies determine the location of maximum SST and hence deep convection (Trenberth, 1997). In the present study, we identify the equatorial western-central Pacific as that region that influences the development of IOZM. Further, we do not rule out the possibility for other external factors involved in triggering the IOZM. For example, Kajikawa et al. (2001) indicated the role of ENSO associated local Hadley circulation in the western Pacific in initiating the SST anomalies in the EEIO through modulation to convection in the maritime continent region. During its mature and peak phases, however, it is quite possible for the IOZM to influence the SOI and ENSO, but our focus here is concentrated in spring season, well before the IOZM is developed.

5. Indonesian Throughflow and the IOZM

Apart from the atmospheric link (Walker circulation), the ITF acts as an oceanic link between the Indian and Pacific Oceans. Therefore, it is instructive to study ITF's role (if any) on the initiation of IOZM. Normally, the ITF brings warm and freshwater from the Pacific to the Indian Ocean which could potentially deepen the thermocline in the Indian Ocean (Wyrtki, 1987; Godfrey, 1996). Therefore, variations in ITF effect the thermal structure and SST in the EEIO.

To get a first-order picture, the correlations between ITF and Z20 (Fig. 15a) and ITF and SST (Fig. 15b) are estimated and values > 0.2 are significant at 95% level. As expected from coastal wave dynamics, the most prominent region of ITF influence on SST and Z20 is noticed off South Java, where the first sign of organized SST variability (Fig. 3c) is observed. The spatial pattern of the correlation along the eastern boundary of the Indian Ocean in Fig. 15a underscores the impact of coastal Kelvin wave dynamics on the ITF transport (e.g. Clark and Liu, 1993, 1994; Yamagata et al., 1996). The interpretation is that changes in the equatorial Indian Ocean winds drive equatorial Kelvin waves, which in turn create coastal Kelvin waves that propagate eastward
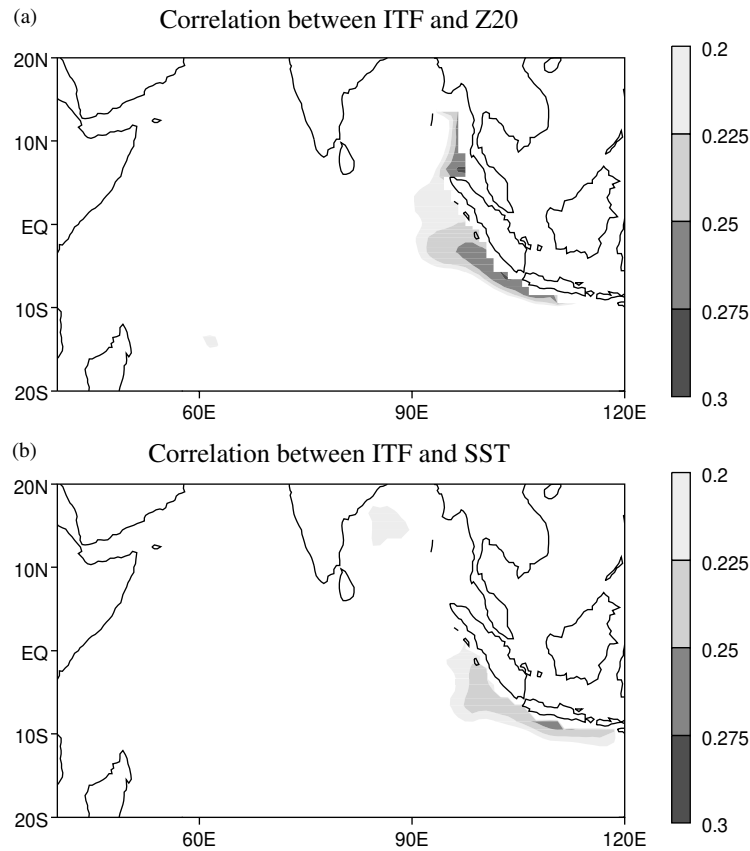
(a)   Correlation between ITF and Z20

(b)   Correlation between ITF and SST

Fig. 15. Correlations between (a) ITF and Z20 and (b) ITF and SST. Values > 0.2 are significant at 95% level.

along the south shore of the Indonesian archipe-
lago. These waves not only affect the along-shore
thermocline off South Java directly, but they also
can cause changes in the thermocline indirectly by
limiting (in the case of downwelling waves) ITF
transport via geostrophic adjustment.

The low-level divergence in the EEIO enhances
the convergence in the WIO and subsequently, the
precipitation increases in the equatorial WIO
between 60–90°E (Fig. 16). Forced by this heat
source, a cyclonic circulation develops in the
lower atmosphere to the north–west of the heating
(Fig. 16) promoting equatorial westerly wind
anomalies. These winds force downwelling Kelvin
waves that propagate along the coast of Java, deepen
the thermocline, and increase sea level. This leads to
a reduction in the ITF (e.g. Potemra et al., 2001).
Through an OGCM experiment, it was shown that
the westerly wind anomalies are indeed the cause for

the reduction in the ITF transport during the early
summer of 1997 (Sprintall et al., 2000).

From the monthly anomalous ITF transport in
strong IOZM years, a composite time series is
constructed. This series is used to estimate the bi-
monthly tendency (January→March→May→
July→September→November→January) in the
ITF transport (Fig. 17). It is clear that there is a
weakening of the transport during spring/early
summer. Thus, once the ITF is weakened, the
thermocline rebounds off Java (Sprintall et al.,
1999) and the prevailing winds (Fig. 12a) help
trigger the IOZM.

6. Interactions between monsoon and IOZM

During spring, the monsoon circulation in the
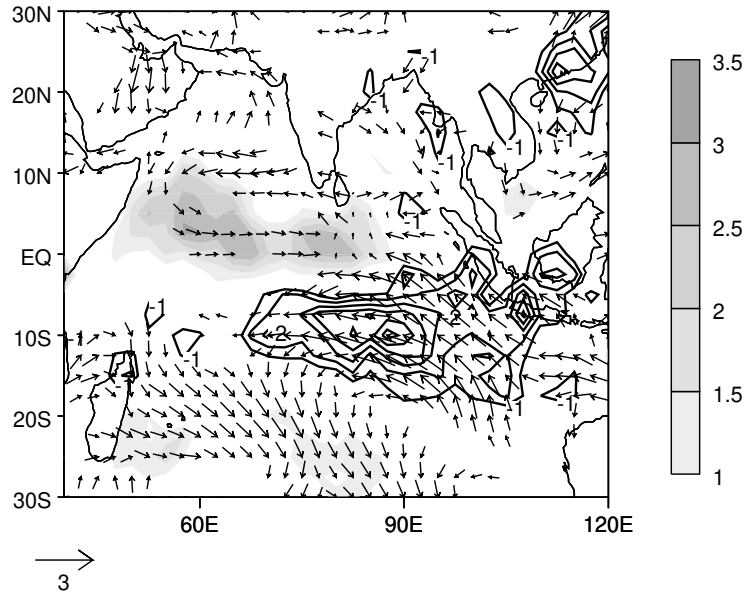Indian Ocean is in its transitional phase and

Fig. 16. April–May composites of anomalous precipitation and surface winds for strong IOZM years. Positive precipitation anomalies are shaded progressively with an interval of 0.5 mm day while negative precipitation anomalies are shown as contours with an interval 0.5 mm/day. The reference wind vector (m/s) is also shown.
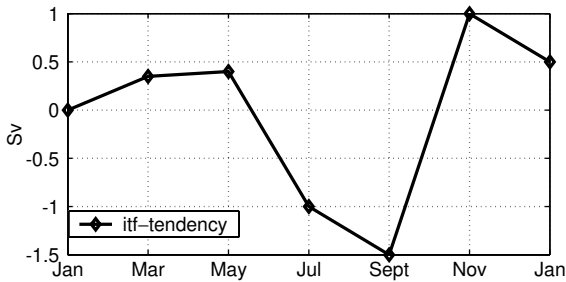

Fig. 17. Bi-monthly composite time series of anomalous ITF transport during strong IOZM years.

therefore weak. However, in the established phases (July–August), it can influence the growth of IOZM (Fig. 3d). On the other hand, Behera et al. (1999) suggested that the above normal Indian summer monsoon rainfall in 1994 was largely due to the cold SSTA in the EEIO. Ashok et al. (2001) extended this idea for other IOZM years. Here, we show the interactive nature between IOZM and monsoon.

Fig. 18a shows the composites of anomalous precipitation and surface winds during July–August of 1982, 1991, 1994 and 1997. The circulation feature and rainfall anomalies over

the Indian sub-continent (not shown) during 1961 and 1967 IOZM years remain similar to Fig. 18a. The negative precipitation anomalies in the EEIO are surrounded by positive precipitation anomalies in the equatorial western-central Indian Ocean and along the entire monsoon trough, from the Indian sub-continent extending eastwards into tropical northwest Pacific. The convergence of air over the Bay of Bengal is due not only to the westerly anomalies but also to southerly flow orginating off Sumatra (Fig. 18a). The inference from Fig. 18a is that the north–south heating (precipitation) gradient over the eastern Indian Ocean favors a local meridional circulation (Gill, 1980; Slingo and Annamalai, 2000), which is instrumental in transporting moisture towards the monsoon trough (Fig. 18b).

The local meridional circulation leads to low-level divergence in the EEIO (Fig. 18b), an aspect noticeable in the total winds (Fig. 18a). Apart from local air–sea interaction, negative precipitation anomalies in the EEIO are also maintained by monsoon-induced subsidence. The twin anticyclones in the rotational component of the wind (Fig. 18c) straddling the EEIO are Rossby-wave
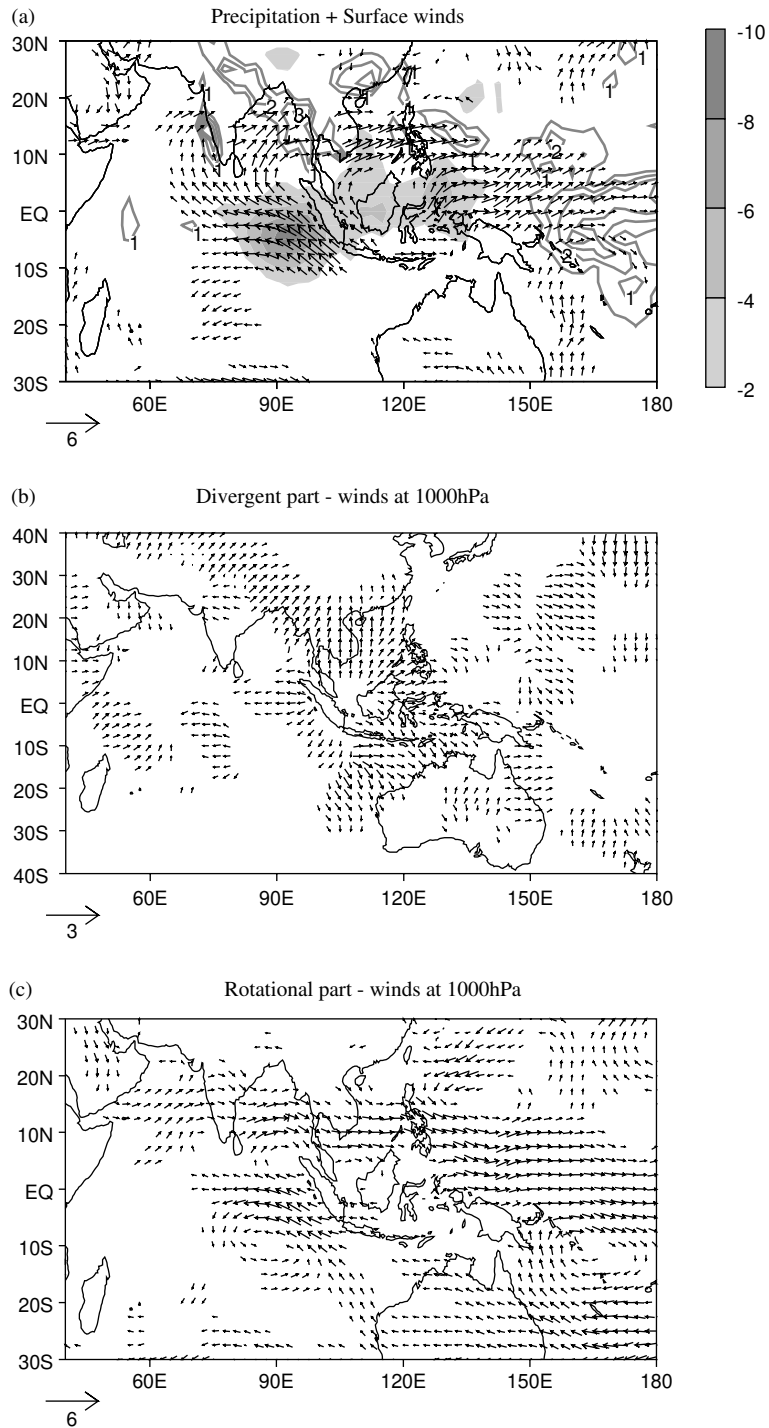
Fig. 18. July–August composites of (a) precipitation and surface winds. Negative (positive) values of precipitation are shaded (contour). The contour interval is 1 mm/day while the shading interval is 2 mm/day; (b) divergent winds and (c) rotational part of the winds at 1000 hPa. Reference vector is shown in all the panels.

response to this heat sink. It is indeed the southern component that enhances the upwelling-favorable winds off Sumatra, leading to northwestward expansion of SSTA (Fig. 3d). Albeit a strong meridional flow, equatorial anomalous easterlies (Fig. 18a) are maintained by air–sea interaction in the EEIO.

7. Summary and discussions

Atmosphere and ocean model assimilated products for the past five decades, in conjunction with observed precipitation and an ocean model estimates of ITF and barrier layer thicknes (BLT), are analyzed to elucidate the role of external (ENSO and ITF) and internal (monsoon) factors in triggering the IOZM, with a focus on air–sea interaction in the EEIO. In particular, we have investigated the cause of anomalous upwelling-favorable winds in boreal spring that lead an IOZM event in the subsequent season. The diagnostics from observations are supplemented with AGCM experiments.

Our major conclusions based on various diagnostics include the following: (a) There exists a natural mode of coupled climate variability in the Indian Ocean that is weak on its own but intensifies under external forcings; (b) Spring to early summer is the 'time window' when the EEIO ocean–atmosphere system is sensistive to these external forcings; (c) Spring precipitation over the EEIO is not related to local SST but appears to be externally controlled; (d) Walker circulation changes induced by developing El Niño or El Niño-like conditions over the west Pacific appear to be one such external forcing to trigger IOZM event; (e) This remote forcing of upwelling-favorable winds off Java is confirmed by sensitivity experiments with an AGCM; (f) In addition, weakened ITF during spring/early summer also may be instrumental to initiating IOZM; (g) an analysis of the heat budget of the mixed layer from an OGCM indicates that cooling off Java in spring is primarily due to entrainment and latent cooling; and (h) once initiated, IOZM interacts with the Asian summer monsoon, giving rise to above normal precipitation during July/August along the monsoon trough, countering the remote effect of El Niño.

The hypothesis that El Niño or El Niño-like conditions trigger the IOZM through changes in Pacific Walker circulation is based on the following findings. From both observations and AGCM experiments, it is shown that spring atmospheric conditions in the Indian Ocean are remotely controlled. Warm SST anomalies and increased precipitation over the equatorial western-central Pacific cause changes in the east–west Walker circulation that ascends over the equatorial west Pacific and descend over the EEIO-maritime continent. The resultant subsidence leads to negative precipitation anomalies over the EEIO and a local heat sink. This probably leads to a chain of ocean–atmosphere processes to initiate an IOZM event: (i) Forced by the heat sink, an anticyclone develops in the lower atmosphere in the southeastern Indian Ocean as a Rossby-wave response. This anticyclone enhances the climatological alongshore upwelling-favorable winds off Java–Sumatra. (ii) The reduction in EEIO precipitation leads to the erosion of the barrier layer, facilitating in the entrainment of cold waters into the mixed layer. (iii) The reduction in ITF transport due oceanic Kelvin waves also help in triggering the IOZM.

In a case study, Ueda and Matsumoto (2001) suggested that El Niño triggered the 1997 IOZM event by increasing the anomalous easterlies in the equatorial Indian Ocean. By analysing a long integration of a coupled GCM, Gualdi et al. (2003) indicated that El Niño could create favorable conditions for the initiation of the IOZM. A major contribution of the present study is the demonstration that suppressed convection and the resultant along-shore winds off the Indonesian coast in *spring* is due to remote forcing from the Pacific, which subsequently triggers pronounced EEIO cooling and a strong IOZM in summer and fall.

During July–August of strong IOZM years, the north–south precipitation (heating) gradient over the eastern Indian Ocean is more dominant than the equatorial east–west heating gradient, resulting in a local meridional circulation with ascend over the monsoon trough and descend in the EEIO.

Thus, in summary heat sink in the EEIO is maintained jointly by local air–sea interaction and monsoon induced anomalous subsidence. As the Rossby-wave response to this heat sink, the rotational winds enhance the alongshore upwelling-favorable winds off Sumatra. Therefore, once triggered by external factors the IOZM grows due to the background monsoon.

The hypothesis proposed in this paper raises the question: Why was the IOZM absent during the developing phase of El Niño prior to 1976? It appears that the warm SSTA of El Niños before 1976 spread westward from the South American coast to central Pacific (Rasmusson and Carpentar, 1982) while in recent decades, the direction of propagation of warm SSTA is eastward from the western-central to eastern Pacific (Wallace et al., 1998; Fedorov and Philander, 2001). This change in the time-space evolution of ENSO leaves different western Pacific SSTA pattern in spring, which we showed to be the key in controlling the spring precipitation in the EEIO. Our recent research indicates that in addition to remote forcing from the Pacific, the phase of the decadal variability in the EEIO thermocline depth is also important for the initiation of the IOZM.

References

Allan, R.J., Chambers, D., Drosdowsky, W., Hendon, H., Latif, M., Nicholls, N., Smith, I., Stone, R., Tourre, Y., 2001. Is there an Indian Ocean dipole, and is it independent of the El Niño-Southern Oscillations? CLIVAR Exchanges 6 (3), 18–22.

Ashok, K., Guan, Z., Yamagata, T., 2001. Impact of the Indian Ocean dipole on the relationship between the Indian monsoon rainfall and ENSO. Geophysical Research Letters 28, 4499–4502.

Baquero-Bernal, A., Latif, M., Legutke, S., 2002. On dipole like variability of sea surface temperature in the tropical Indian Ocean. Journal of Climate 15, 1358–1368.

Behera, S.K., Krishnan, R., Yamagata, T., 1999. Unusual Ocean–atmosphere conditions in the tropical Indian Ocean during 1994. Geophysical Research Letters 26, 3001–3004.

Birkett, C., Murtugudde, R., Allan, J.A., 1999. Indian Ocean climate event brings floods to East Africa's Lakes and the Sudd Marsh. Geophysical Research Letters 26, 1031–1034.

Bjerknes, J., 1969. Atmospheric teleconnections from the equatorial Pacific. Monthly Weather Review 97, 163–172.

Carton, J.A., Chepurin, G., Cao, X., Giese, B., 2000. A simple ocean data assimilation analysis of the global upper ocean 1950–95. Part I: methodology. Journal of Physical Oceanography 30, 294–309.

Chambers, D.P., Tapley, B.D., Stewart, R.H., 1999. Anomalous warming in the Indian Ocean coincident with El Niño. Journal of Geophysical Research 104, 3035–3047.

Chen, D., Rothstein, L.M., Busalacchi, A.J., 1994. A hybrid vertical mixing scheme and its application to tropical ocean models. Journal of Physical Oceanography 24, 2156–2179.

Clark, A.J., Liu, X., 1993. Observations and dynamics of semiannual and annual sea levels near the eastern equatorial Indian Ocean boundary. Journal of Physical Oceanography 23, 386.

Clark, A.J, Liu, X., 1994. Interannual sea level in the northern and eastern Indian Ocean. Journal of Physical Oceanography 24, 1224–1235.

Deser, C., Wallace, J.M., 1987. El Niño events and their relation to the Southern Oscillation: 1925–1986. Journal of Geophysical Research 92, 14189–14196.

Flohn, H., 1987. Indonesian droughts and their teleconnections. Ber. Geogr. Stud. 20, 251–265.

Fedorov, A.V., Philander, G.H., 2001. A stability analysis of tropical ocean atmosphere interactions: bridging measurement and theory for El Niño. Journal of Climate 14, 3086–3101.

Feng, M., Meyers, G., Wijffels, S., 2001. Interannual upper ocean variability in the tropical Indian Ocean. Geophysical Research Letters 28, 4151–4154.

Gill, A.E., 1980. Some simple solutions for heat induced tropical circulation. Quarterly Journal of the Royal Meteorological Society 106, 447–462.

Godfrey, J.S., 1996. The effect of the Indonesian Throughflow on ocean circulation and heat exchange with the atmosphere: a review. Journal of Geophysical Research 101, 12217–12238.

Graham, N.E., Barnett, T.P., 1987. Sea surface temperature, surface wind divergence, and convection over tropical oceans. Science 258, 657–659.

Gualdi, S., Guilyardi, E., Navarra, A., Masina, S., Delecluse, P., 2003. The interannual variability in the tropical Indian Ocean. Climate Dynamics 20, 567–582.

Hastenrath, S., 2002. Dipoles, temperature gradients and tropical climate anomalies. Bulletin of the American Meteorological Society 83, 735–738.

Hastenrath, S., Nicklis, A., Greischar, L., 1993. Atmospheric–hydrospheric mechanisms of climate anomalies in the western equatorial Indian Ocean. Journal Geophysical Research 98 (C11), 20219–20235.

Huang, B., Kinter, J.L., 2002. The interannual variability in the tropical Indian Ocean and its relations to El Niño-Southern Oscillation. Journal of Geophysical Research, 107, C11, 3199 (doi: 10.1029/2001JC001278).

Iizuka, S., Matsuura, T., Yamagata, T., 2000. The Indian Ocean SST dipole simulated in a coupled general circulation model. Geophysical Research Letters 27, 3369–3372.

Kajikawa, Y., Yasunari, T., Kawamura, R., 2001. The role of local Hadley circulation over the western Pacific on the zonally asymmetric anomalies over the Indian Ocean. Journal of the Meteorological Society of Japan, in press.

Kalnay, E., et al., 1996. The NCEP/NCAR 40 year reanalysis project. Bulletin of the American Meteorological Society 77, 437–471.

Kapala, A., Born, K., Flohn, H., 1994. Monsoon anomaly or an El Niño event at the equatorial Indian Ocean? Catastrophic rains 1961/62 in East Africa and their teleconnections. In: Proceedings of the International Conference on Monsoon Variability and Prediction, Trieste, Italy, pp. 119–126.

Klein, S.A., Soden, B.J., Lau, N.C., 1999. Remote sea surface temperature variations during ENSO: evidence for a tropical atmospheric bridge. Journal of Climate 12, 917–932.

Latif, M., Barnett, T., 1995. Interactions of the tropical oceans. Journal of Climate 8, 952–964.

Latif, M., Dommenget, D., Dima, M., Grotzner, A., 2000. The role of Indian Ocean sea surface temperature in forcing east African rainfall anomalies during December–January 1997/98. Journal of Climate 12, 3497–3504.

Lau, N.C., Nath, M.J., 2001. Impact of ENSO on the variability of the Asian–Australian monsoon as simulated in GCM experiments. Journal of Climate 13, 4287–4309.

Le Blanc, J.L., Boulanger, J.P., 2001. Propagation and reflection of long equatorial waves in the Indian Ocean from TOPEX/POSEIDON data during the 1993–1998 period. Climate Dynamics 17, 547–557.

Masson, S., Delecluse, P., Boulanger, J.P., Menkes, C., 2002. A model study of the seasonal variability and formation mechanisms of barrier layer in the eastern equatorial Indian Ocean. Journal of Geophysical Research, 107, C12 (doi: 10.1029/2001JC00832).

Matsuno, T., 1966. Quasi-geostrophic motions in the equatorial area. Journal of Meteorological Society of Japan 44, 25–43.

McCreary, J.P., Kundu, P., 1989. A numerical investigation of sea surface temperature variability in the Arabian Sea. Geophysical Research 94, 16097–16114.

Meyers, G., 1996. Variation of Indonesian Throughflow and the El Niño-Southern oscillation. Journal of Geophysical Research 101, 12255–12263.

Murtugudde, R., Busalacchi, A.J., 1999. Interannual variability of the dynamics and thermodynamics of the tropical Indian Ocean. Journal of Climate 12, 2300–2326.

Murtugudde, R., Seager, R., Busalacchi, A.J., 1996. Simulation of the tropical oceans with an ocean GCM coupled to an atmospheric mixed layer model. Journal of Climate 9, 1795–1815.

Murtugudde, R., Goswami, B.N., Busalacchi, A.J., 1998a. Air–sea interaction in the southern tropical Indian Ocean and its relations to interannual variability of the monsoon over India. Proceedings of the International Conference on Monsoon and Hydrologic Cycle, Kyongju, Korea. 22–25 April, 1998.

Murtugudde, R., Busalacchi, A.J, Beauchamp, J., 1998b. Seasonal to interannual effects of the Indonesian Throughflow on the tropical Indo-Pacific basin. Journal of Geophysical Research 103, 21425–21441.

Murtugudde, R., McCreary, J.P., Busalacchi, A.J., 2000. Oceanic processes associated with anomalous events in the Indian Ocean with relevance to 1997–1998. Journal of Geophysical Research 105, 3295–3306.

Nicholls, N., Drosdowsky, W., 2001. Is there an equatorial Indian Ocean SST dipole, independent of the El Niño Southern Oscillation? 81st American Meteorological Society, Annual Meeting, Albuquerque, NM, USA, 14–19 January 2001.

Philander, G., 1990. El Niño and Southern Oscillation. Academic Press, New York, 293pp.

Potemra, J.T., Hautala, S.L., Sprintall, J., Pandoe, W., 2001. Interaction between the Indonesian Seas and the Indian Ocean in observations and numerical models. Journal of Physical Oceanography 32, 1838–1854.

Rao, R.R., Molinari, R.L., Fiesta, J.F., 1989. Evolution of the climatological near-surface thermal structure of the tropical Indian Ocean: 1. description of mean monthly mixed layer depth, and sea surface temperature, surface current, and surface meteorological fields. Journal of Geophysical Research 105, 985–1015.

Rao, S.A., Behera, S.K., Masumotto, Y., Yamagata, T., 2002. Interannual subsurface variability in the tropical Indian Ocean (with a special emphasis on the Indian Ocean dipole). Deep-Sea Research II 49, 1549–1572.

Rasmusson, E.M., Carpentar, T.H., 1982. Variations in tropical sea surface temperature and surface wind fields associated with the Southern Oscillatoion/El Niño. Monthly Weather Review 110, 354–384.

Reverdin, G., Cadet, D., Gutzler, D., 1986. Interannual displacements of convection and surface circulation over the equatorial Indian Ocean. Quarterly Journal of the Royal Meteorological Society 112, 43–46.

Roeckner, et al., 2001. The ECHAM5.1 Atmospheric General Circulation Model. Rep. 101, Max-Planck-Institut fur Meteorologie, Hamburg, Germany.

Saji, N.H., Goswami, B.N., Vinayachandran, P.N., Yamagata, T., 1999. A dipole mode in the tropical Indian Ocean. Nature 401, 360–363.

Schiller, A., Godfrey, J.S., McIntosh, P.C., Meyers, G., Fielder, R., 2000. Interannual dynamics and thermodynamics of the Indo-Pacific Oceans. Journal of Physical Oceanography 30, 987–1012.

Schott, F., 1983. Monsoon response of the Somali current and associated upwelling. Progress in Oceanography 12, 357–381.

Schott, F., McCreary, J.P., 2001. The monsoon circulation of the Indian Ocean. Progress in Oceanography 51, 1–123.

Shukla, J., 1998. Predictability in the midst of Chaos: a scientific basis for climate forecasting. Science 282, 728–731.

Slingo, J.M., Annamalai, H., 2000. 1997. The El Niño of the century and the response of the Indian summer monsoon. Monthly Weatherly Review 128, 1778–1797.

Soman, M.K., Slingo, J.M., 1997. Sensitivity of the Asian summer monsoon to aspects of sea surface temperature anomalies in the tropical Pacific Ocean. Quarterly Journal of the Royal Meterological Society 123, 309–336.

Sprintall, J., Tomczak, M., 1992. Evidence of the barrier layer in the surface layer of the tropics. Journal of Geophysical Research 97, 7305–7316.

Sprintall, J., Chong, J., Syamusdin, F., Morawitz, W., Hautala, S., Bray, N., Wijffels, S., 1999. Dynamics of the South Java current in the Indo-Australian basin. GeoPhysical Research Leters 26, 2493–2496.

Sprintall, J., Gordon, A., Murtugudde, R., Susanto, D., 2000. An Indian Ocean Kelvin wave observed in the Indonesian seas during May 1997. Journal of Geophysical Research 105, 17217–17230.

Trenberth, K.E., 1997. The definition of El Niño. Bulletin of the American Meteorological Society 78, 2771–2777.

Trenberth, K.E., Stepaniak, D.P., Caron, J.M., 2000. The global monsoons as seen through the divergent atmospheric circulation. Journal of Climate 13, 3969–3993.

Ueda, H., Matsumoto, J., 2001. A possible triggering process of east–west asymmetric anomalies over the Indian Ocean in relation to 1997/98 El Niño. Journal of Meteorological Society of Japan 78, 803–818.

US CLIVAR Asian–Australian Monsoon Research Prospects, 2001. Available at http://www.usclivar.org.

Venzke, S., Latif, M., Vilwock, A., 2000. The coupled GCM ECHO-2, II, Indian Ocean response. Journal of Climate 13, 1371–1383.

Wallace, J.M., Rasmusson, E.M., Mitchell, T.P., Kousky, V.E., Sarachik, E.S., von Storch, H., 1998. On the structure and evolution of ENSO-related climate variability in the tropical Pacific: lessons from TOGA. Journal of Geophysical Research 103, 14241–14259.

Wang, C., Weisberg, R.H., 2000. The 1997-98 El Niño evolution relative to previous El Niño events. Journal of Climate 13, 488–501.

Webster, P.J., 1972. Response of the tropical atmosphere to local steady flow. Monthly Weatherly Review 100, 518–541.

Webster, P.J., Magana, O., Palmer, T.N., Shukla, J., Thomas, R.A., Yanai, M., Yasunari, T., 1998. Monsoons: processes, predictability, and the prospects for prediction. Journal of Geophysical Research 103, 14451–14510.

Webster, P.J., Moore, A.M., Loschnigg, J.P., Leben, R.R., 1999. Coupled oceanic-atmospheric dynamics in the Indian Ocean during 1997–98. Nature 401, 356–360.

Wyrkti, K., 1987. Indonesian Throughflow and the associated pressure gradient. Journal of Geophysical Research 92, 12941–12946.

Xie, S.P., 1995. Interaction between the annual and interannual variations in the equatorial Pacific. Journal of Physical Oceanography 25, 1930–1941.

Xie, P., Arkin, P., 1996. Analyses of global monthly precipitation using gauge observations, satellite estimates, and numerical model predictions. Journal of Climate 9, 840–858.

Xie, S.P., Annamalai, H., Schott, F.A., McCreary, J.P., 2002. Structure and mechanisms of south Indian Ocean climate variability. Journal of Climate 15, 867–878.

Yamagata, T., Mizuno, K., Masumoto, Y., 1996. Seasonal variations in the equatorial Indian Ocean and their impact on the Lombok Throughflow. Journal of Geophysical Research 101, 12465–12473.

Yamagata, T., Behera, S., Rao, S.A., Guan, Z., Ashok, K., Saji, H., 2002. The Indian Ocean dipole: a physical entity. CLIVAR exchanges 24, 15–18.

Yu, L., Rienecker, M., 1999. Mechanisms for the Indian Ocean warming during the 1997–98 El Niño. Geophysical Research Letters 26, 735–738.

Yu, L., Rienecker, M., 2000. Indian Ocean warming of 1997–1998. Journal of Geophysical Research—Oceans 105, 16923–16939.